Lipopolysaccharides at Solid and Liquid Interfaces: Models for Biophysical Studies of the Gram-negative Bacterial Outer Membrane

Nicoló Paracini, Emanuel Schneck, Anne Imberty, Samantha Micciulla

Lipopolysaccharides at Solid and Liquid Interfaces: Models for Biophysical Studies of the Gram-negative Bacterial Outer Membrane

Nicoló Paracini,*,† Emanuel Schneck,‡ Anne Imberty,¶ and Samantha Micciulla*,§

†*Malmö University, Malmö, Sweden*

‡*Physics Departent, Technische Universität Darmstadt, Darmstadt, Germany*

¶*Université Grenoble Alpes, CNRS, CERMAV, Grenoble, France*

§*Institut Laue-Langevin, Grenoble, France*

E-mail: nicolo.paracini@mau.se; micciulla@ill.fr

Lipopolysaccharides (LPSs) are a constitutive element of the cell envelope of Gram-negative bacteria, representing the main lipid in the external leaflet of their outer membrane (OM) lipid bilayer. These unique surface-exposed glycolipids play a central role in the interactions of Gram-negative organisms with their surrounding environment and represent a key element for protection against antimicrobials and the development of antibiotic resistance. The biophysical investigation of a wide range of different types of *in vitro* model membranes containing reconstituted LPS has revealed functional and structural properties of these peculiar membrane lipids, providing molecular-level details of their interaction with antimicrobial compounds. LPS assemblies reconstituted at interfaces represent a versatile tool to study the properties of the Gram-negative OM by exploiting several surface-sensitive techniques, in particular X-ray and neutron scattering, which can probe the structure of thin films with sub-nanometer resolution. This review provides an overview of different ap-

proaches employed to investigate structural and biophysical properties of LPS, focusing on studies on Langmuir monolayers of LPS at the air/liquid interface and a range of supported LPS-containing model membranes reconstituted at solid/liquid interfaces.

Contents

Keywords: Lipopolysaccharides, outer membrane, X-ray and neutron scattering, model bacterial interfaces, antimicrobial peptides

1 Introduction

Despite the extremely diversified range of environments that cells interact with, the phospholipid bilayer has affirmed itself as life's interface of choice. In Gram-negative bacteria, however, the plasma membrane and the surrounding peptidoglycan cell wall, are enclosed by an additional outer membrane (OM) with a distinctive asymmetric bilayer structure comprising an inner leaflet of glycerophospholipids and an outer leaflet of characteristic lipopolysaccharides (LPSs)[1–3] (Figure 1). Due to its peripheral location, at the interface between the bacterial cell and its surroundings, LPS plays key roles in the interaction with hosts, commensal and competing organisms as well as protecting Gram-negative organisms from noxious external agents, including antibiotics. Its unique molecular structure and exclusive presence on the Gram-negative bacterial surface render LPS a target for recognition by the immune systems of plants, animals and humans.[3,4] At the same time, the remarkably low permeability of the LPS layer towards hydrophobic compounds, which can normally diffuse through phospholipid membranes, is one of the main advantages that enable Gram-negative pathogens to evade the effects of antimicrobials, establishing the basis of their growing antibiotic resistance. [5,6]

The central role of LPS as a fundamental component of the OM has driven intense research

efforts aimed at understanding how the physico-chemical properties of this multifaceted molecule contribute to the barrier function of the OM. Whilst crystallographic data elucidated the structure of individual LPS molecules in complex with OM proteins, surface sensitive techniques, particularly neutron and X-ray scattering, shed light on the properties and behaviour of LPS reconstituted at air/liquid and solid/liquid interfaces. As a result, a number of LPS-containing models of the OM have been developed and characterised, providing an extensive toolbox for the investigation of biophysical aspects of the main lipid component of the Gram-negative bacterial surface. This review is divided in two sections: the first part provides a general overview of LPS in its biological context, as a constitutive element of the OM permeability barrier and as the binding partner of a range of membrane and soluble proteins; the second section focuses on the results obtained by biophysical studies performed on different types of LPS reconstituted at air/liquid and solid/liquid interfaces to model the Gram-negative OM, followed by an overview of simulation-based theoretical studies of LPS assemblies.

2 Biological context

The unique properties of the Gram-negative OM rely on the asymmetric lipid distribution within its bilayer structure, with LPS localised in the external leaflet of the membrane.[2] LPS is essential for nearly all Gram-negative bacteria, with the notable exceptions of a restricted number of organisms.[7,8] The widespread reliance of Gram-negative organisms on this unique family of glycolipids has its roots on both the structural and functional roles that these molecules play in the OM. Here we outline a summary of the main biological aspects of LPS which provide some of the background necessary to contextualise the results of biophysical studies on LPS at solid and liquid interfaces.

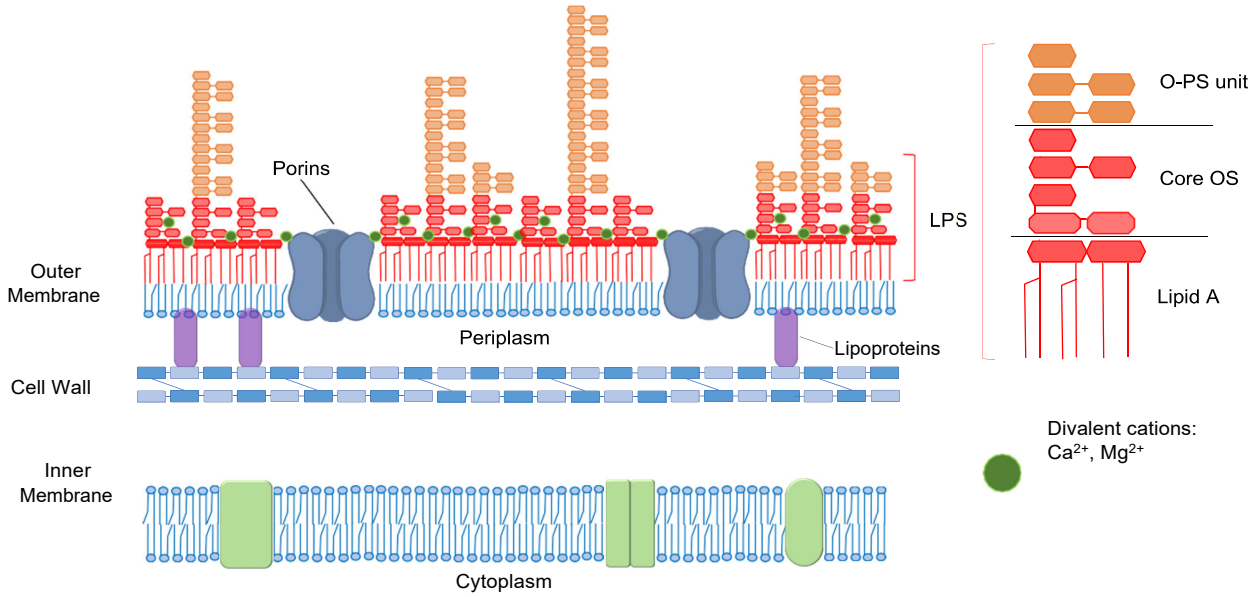

Figure 1: Double membrane structure of the Gram-negative bacterial cell envelope. LPS is localised in the outer leaflet of the outer membrane, at the interface between the cell and the external environment. Divalent cations bridge the negative charges of neighbouring LPS molecules, stabilising the OM. Porins are the most abundant family of OM proteins, consisting of mono- or trimeric OM-spanning β-barrels.

2.1 Chemical structure of LPS

Although the LPS molecule displays variability, depending on the species and the conditions of growth,[9,10] its basic amphiphilic structure is typically divided into three chemically distinct domains: *(i)* the acylated lipid A region which forms the hydrophobic lipid matrix of the outer leaflet of the OM, and the hydrophilic *(ii)* core oligosaccharide (core OS) and *(iii)* O-antigen polysaccharide (O-PS) regions which make up the polar head group of the molecule and extends towards the external environment on the bacterial surface (Figure 1). The lipid A moiety tipically consists of a central disaccharide of glucosamine (GlcN), phosphorylated on the position 1 and 4′, which carries four acyl chains linked via ester bonds at position 3 and 3′ and via amide bonds at position 2 and 2′. In the model organism *Escherichia coli* grown in standard laboratory conditions (Luria-Bertani broth at 37°C) the four saturated acyl chains are 3-hydroxymyristoyl (C14:0) moieties, two of which are further esterified with secondary lauroyl (C12:0) and myristoyl chains on the non-reducing end

of the GlcN backbone, yielding a hexa-acylated lipid A[4](Figure 2a). Lipid A is the most structurally conserved part of LPS and its hexa-acylated and bi-phosphorylated form is a strong agonist of TLR4 receptors, making it one of the most potent activators of the innate immune system of animals and plants.[11,12] Despite being highly conserved, a series of lipid A structures that deviate from the *E. coli* paradigm have been characterised and are reviewed in Ref 4.

The hydroxyl group at position 6' of the GlcN links lipid A with the core OS region comprising a branched oligosaccharide of 10-12 sugars.[13,14] The core OS domain can be further divided into an inner core region, proximal to the lipid A and composed of distinctive heptose residues bearing anionic phosphate groups and carboxylic acid moieties, and a distal outer core region typically containing non-charged hexose sugars.[14] The inner core OS is typically linked to the lipid A via a di- or tri- saccharide of 3-deoxy-manno-oct-2-ulosonic acid (Kdo) residues which is a hallmark of the LPS molecule. In *E. coli* there are 5 different types of core regions, R1-R4 and K12 which display some degree of variability in the composition and connection of the monosaccharides (Figure 2b, c).

In many Gram-negative species (e.g. members of *Enterobacteriaceae*) the terminal part of the LPS structure is a polymer of identical repeating oligosaccharide units forming the O-antigen polysaccharide (O-PS) chain.[15,16] When present, the degree of polymerisation (i.e. the number of repeating oligosaccharide units) of the O-PS chain is highly variable within single organisms which contain in their OM LPS molecules with a number of O-antigen units between zero and several dozens, in some cases exceeding 100 units.[17] Together with its significantly heterogeneous length, the O-PS is also the most chemically diverse of the three LPS domains with more that 180 variants in *E. coli* alone.[15] Its basic repeat units are typically formed of two to seven monosaccharides (or sugar derivatives), which can be linear or branched, and bear a variety of functional groups including anionic substituents which confer an overall negative charge to the O-PS chains, as in some *Pseudomonas aeruginosa*[18] and *E. coli*[15] species.

For an in-depth and thorough overview on the chemical aspects of LPS the reader is referred to the recent review by DiLorenzo *et al* .[3]

2.1.1 LPS nomenclature

LPS chemotypes that share structural similarities are identified with a common nomenclature. Rough LPS refers to LPS that lacks the O-PS domain and is therefore composed of the lipid A and core OS regions only. In *E. coli* and *Salmonella*, rough LPS with a complete core structure is termed RaLPS whilst mutants that synthesise an incomplete (i.e. truncated) version of the core region are named Rc, Rd and ReLPS chemotypes. The latter is sometimes referred to as "deep rough" LPS and corresponds to the Kdo_2-lipid A structure, which is the minimal viable form of LPS in most Gram-negative bacteria, [8] whilst RcLPS contains the complete heptose region of the inner core OS.[19] Most laboratory adapted strains (e.g. *E. coli* K12) have lost the ability to synthesise the O-PS, and therefore produce rough LPS.[20] Smooth LPS, on the other hand, refers to LPS produced by bacteria capable of synthesising and attaching the O-PS domain to the rough LPS scaffold. Given the remarkable size polydispersity of these molecules, resulting from the highly variable degree of polymerisation of the O-antigen units, the term "smooth LPS" defines a highly heterogeneous group of molecules that can span a size range between 4 and up to more than 50 kDa. [16,21] It's important to note that as a consequence of this variability, smooth LPS generally contains a considerable fraction of rough LPS molecules that completely lack the O-antigen. It has been estimated that smooth LPS contains up to 60% molar fraction of short LPS molecules bearing either no or a single O-antigen unit.[21] The smooth and rough terminologies derive from the appearance on solid media of the edges of bacterial colonies that express the respectively named types of LPS.[22] The term "wild-type" LPS denotes the naturally occurring phenotype expressed by a particular organism. In the case of enteric species, wild-type LPS often corresponds to smooth LPS, however the two definitions are not synonymous. "Semi-rough" LPS is sometimes used to indicate LPS bearing a single O-antigen repeat unit whilst

the term lipooligosaccharide (LOS) identifies the rough LPS scaffold modified with one or a few extra monosaccharides that are not related to the O-antigen, often found in the OM of mucosal pathogens. [16]

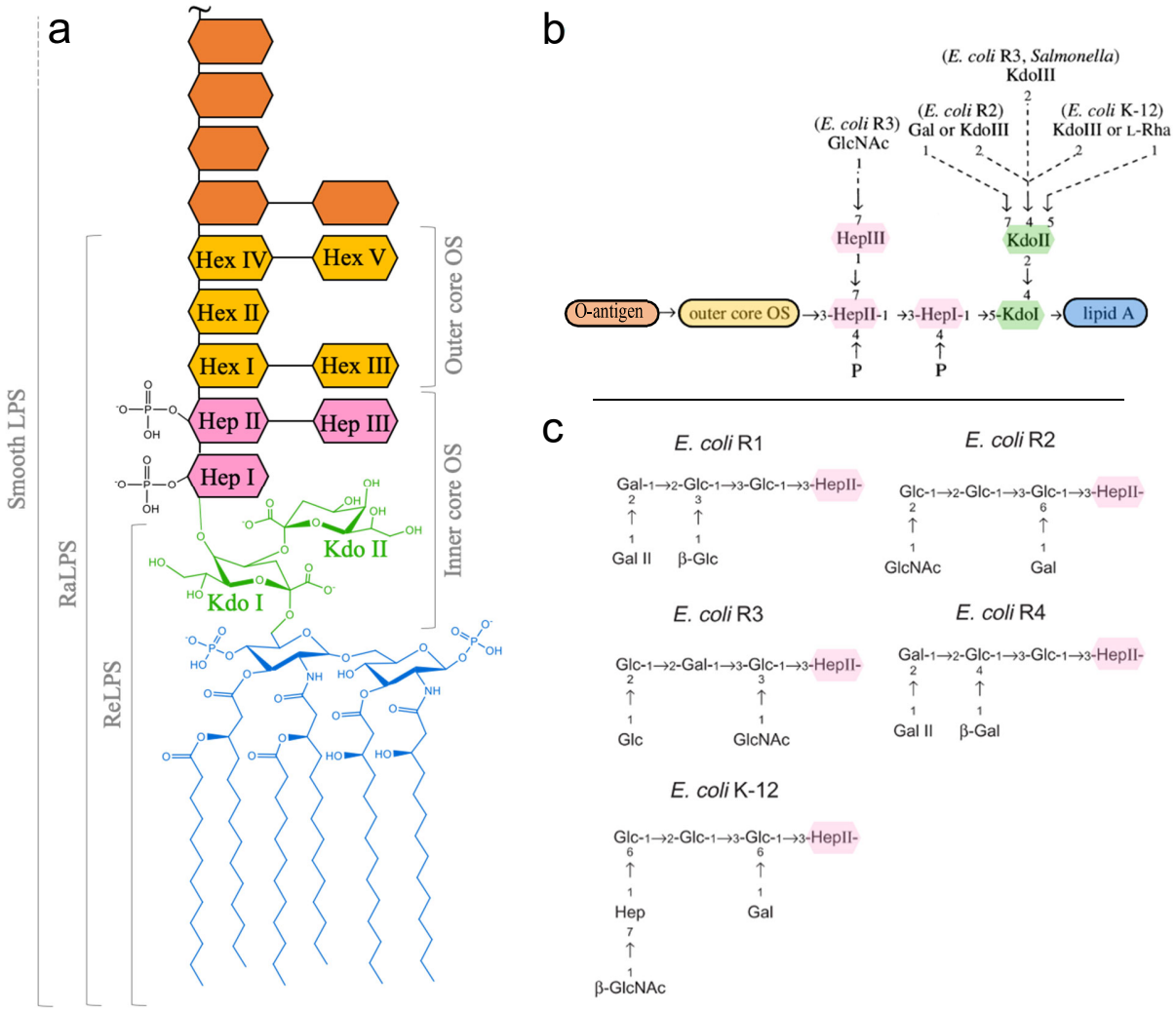

Figure 2: Structure of *E. coli* LPS and variability of the core OS region. **a)** Schematic structure of LPS. The hydrophobic lipid A (blue) anchors LPS to the OM. The core oligosaccharide is divided into an inner and an outer region containing the Kdo disaccharide (green) linked to heptose residues (pink) in the inner core, whilst the outer core is composed by hexose residues (yellow). The O-antigen unit (orange) has a variable structure and forms the repeating oligosaccharide that constitute the O-PS chain, which is typically polydisperse as the number of repeating units varies greatly. **b)** Inner core variability in *E. coli*. **c)** Outer core variability in *E. coli*. Dashed lines indicate non-stochiometric substitutions. Glc = glucose, Gal = galactose, GlcNAc = acetylglucosamine. Hep = heptose, Kdo = 3-deoxy-D-manno-oct-2-ulosonic acid, Rha = rhamnose. Adapted from Ref. 13.

2.2 LPS synthesis and transport

The localisation of LPS in the outer leaflet of the OM is the result of a series of synthetic steps, the Raetz pathway, coupled to a complex transport system that spans the periplasm and ultimately delivers LPS molecules to the outer leaflet of the OM[2,23](Figure 3a). The Raetz pathway begins in the cytoplasm with a sequence of soluble enzymes which produce the Kdo_2-lipid A moiety.[24] The core OS is then assembled in a stepwise manner on the cytoplasmic side of the inner membrane (IM) by a series of glycosyltransferases which sequentially add monosaccharides to the nascent core OS.[10,13,25] Due to the strictly sequential nature of the core OS synthesis, it is possible to engineer bacteria into producing rough LPS with well-defined core OS structures by silencing the expression of target genes responsible for the core OS assembly, which leads to the production of truncated versions of rough LPS[26,27] (Figure 3b).

Once the synthesis of the core OS is terminated, rough LPS molecules are flipped by the IM-embedded protein MsbA to the periplasmic side of the IM.[28] Here, in smooth strains, the O-PS chain which is synthesised separately, is linked to the core OS by the O-antigen ligase WaaL, a membrane protein embedded in the IM.[29] The final length of the O-PS chains can vary greatly and the mechanisms regulating its size distribution have been recently reviewed by Whitfield *et al* .[16] Finally, fully synthesized LPS molecules are transported across the periplasm to the OM by a complex machinery of seven proteins (LptA to LptG), which leads to the delivery of LPS to the outer leaflet of the OM (Figure 3). The physical bridge which delivers LPS molecules to the OM is formed by LptA proteins,[30] which span the periplasm and connects the IM-bound $LptB_2FGC$ complex[31,32] to the LptDE proteins, which insert LPS in the OM.[33]

After the delivery to its final location on the outer leaflet of the OM, LPS is subject to further remodelling of its structure, operated by dedicated OM enzymes, reviewed in Ref. 8 and 25. LPS remodelling is primarily directed to the lipid A moiety of LPS in order to alter the physico-chemical properties of the OM in response to environmental stimuli. The most

common forms of LPS remodelling comprise variations of the acylation pattern by addition or removal of alkyl chains of the lipid A and reduction of its net negative charge by addition of positively charged phosphorylethanolamine or aminoarabinose to the phosphate groups present on the GlcN backbone.[25]

A crucial aspect of the OM is the lipid asymmetry between the inner phospholipid leaflet and the outer LPS layer which is actively maintained by dedicated OM proteins, reviewed in Ref. 2. These include the maintenance of lipid asymmetry (Mla) family of proteins,[34] and the OM enzymes PldA and PagP,[2] which contribute to the elimination of misplaced phospholipids that end up in the LPS leaflet and can compromise the integrity of the OM. A detailed and comprehensive description of the assembly and maintenance of lipids in the OM can be found in the recent review by Lundsted *et al* [35]

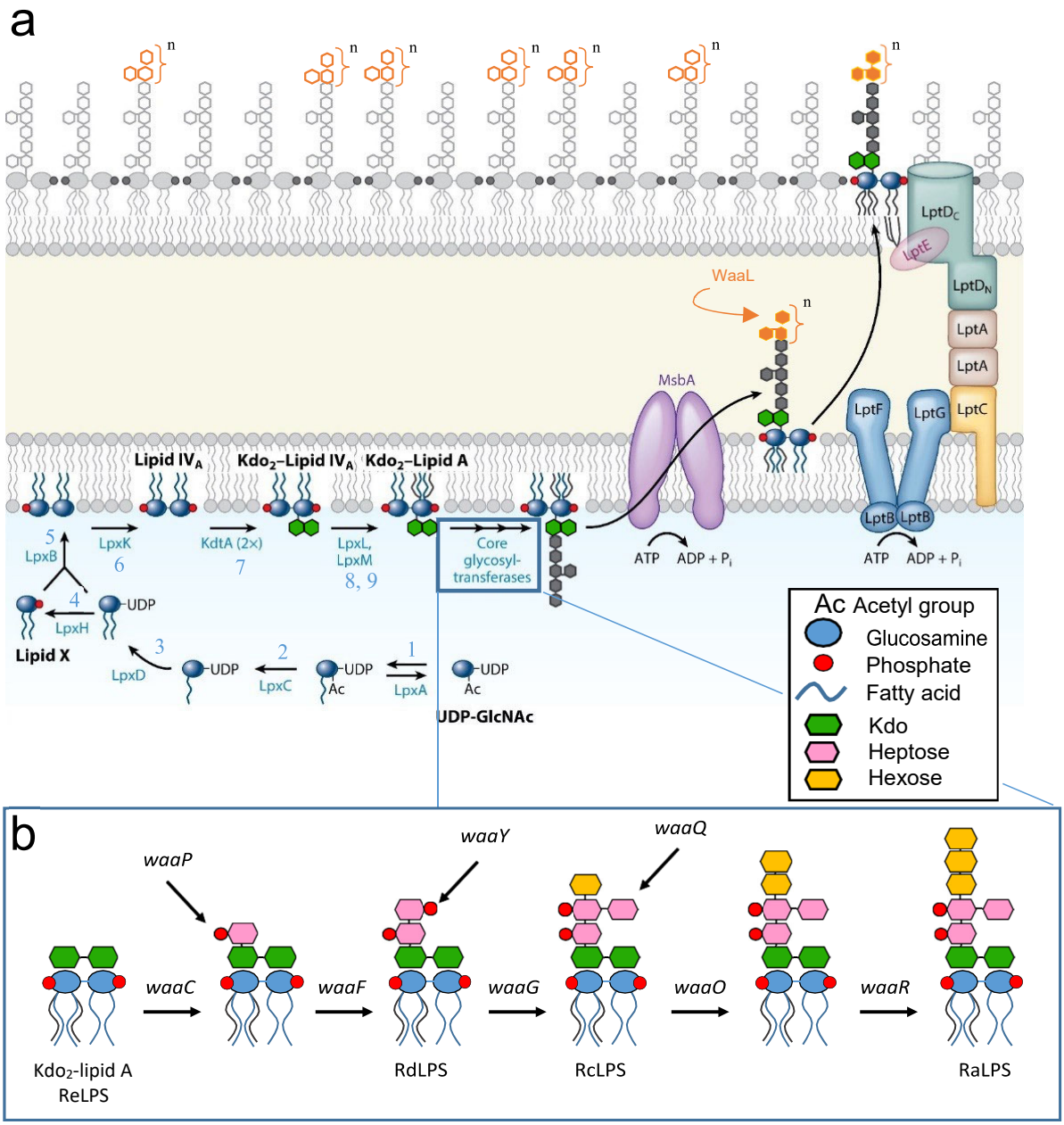

Figure 3: Synthesis and transport of LPS **(a)** Biosynthetic pathway of LPS. The 9 enzymatic steps (numbered in blue) of the Raetz pathway lead to the synthesis of the Kdo2-lipid A unit. Once the core oligosaccharide is assembled (shown in **b**) LPS is flipped to the periplasmic side of the IM by MsbA, linked to the O-antigen polysaccharide by the IM-bound ligase WaaL and transported to the outer leaflet of the OM by the 7-protein Lpt complex. Adapted from Ref. 2. **(b)** Assembly of the core oligosaccharide residues. The genes encoding the enzymes responsible for the addition of the individual residues are labelled. The *waa* locus is also known as *rfa* (redrawn from Ref. 36).

2.3 Barrier properties of the OM

The OM provides Gram-negative bacteria with a remarkably effective defence barrier against penetration of harmful molecules. The layer of tightly packed LPS molecules that make up its outer leaflet renders the diffusion of hydrophobic compounds up to two orders of magnitude slower than through canonical phospholipid bilayers. [37] This extremely limited permeability through the LPS layer constitutes the basis of the OM barrier properties and represents one of the most important limitations to the development of novel antibiotics active against Gram-negative bacteria.[38]

Due to the polyanionic nature of lipid A and the inner core OS, the integrity of the LPS layer, and therefore of the OM, relies upon the presence of divalent cations (Ca^{2+} and Mg^{2+}) which act as bridges between the negative charges of neighbouring LPS molecules.[39] The central role of divalent cations for the integrity of the OM has been known since the early investigations on the Gram-negative cell envelope pioneered by Leive and co-workers, who were the first to study the permeabilising effect of EDTA, linking the destabilisation of the LPS layer to the removal of Ca^{2+} and Mg^{2+} by this chelating agent.[40–42] The role of divalent cations is not limited to the cross-linking of LPS molecules into a tight network but has also been shown in numerous studies to be crucial for LPS-protein interactions. [43–47]

2.3.1 Routes across the OM

The impermeable nature of the OM implies a tight association between LPS and proteins embedded in the OM, which in some organisms have been suggested to cover more than half of the Gram-negative cell surface.[48] Recent atomic force microscopy data has provided some of the highest resolution images of the OM of whole *E. coli* cells, showing how the OM resembles a mosaic of coexisting phase separated LPS-rich and OM proteins-rich regions which are essential to its barrier function.[49] Porins are the most prominent family of OM proteins, consisting of water-filled β-barrel channels that traverse the OM and allow diffusion of small hydrophilic solutes with a size limit of around 700 Da.[50,51] Due to the combination of the im-

permeable LPS lipid matrix and the relatively low solute specificity of major Gram-negative porins such as OmpF, the OM has often been compared to a molecular sieve, a concept first introduced in the early studies of OM permeability by Nikaido and co-workers.[52] The molecular sieve properties of the OM are now recognised as the major hurdle to overcome in the development of new antibiotics active against Gram-negative pathogens.[6,53,54] Because of these OM-imposed limitations, clinically approved antimicrobial compounds active against Gram-negative bacteria are on average smaller and more hydrophilic than those active against Gram-positives, with a very evident cutoff at around 700 Da, a direct consequence of the requirement to cross the OM via the tight lumen of water-filled porin channels[5] (Figure 4). The porin route, imposed on antibiotics by the impermeable LPS barrier, does not only represent a restriction to the physico-chemical properties of effective antimicrobials but also enhances resistance strategies such as the expression of efflux pumps which effectively eliminate harmful compounds even after they reach the periplasmic space.[55,56] For an in-depth description of the role of porins in antibiotic permeation the reader is referred to the recent review by Prajapati *et al*, which addresses practical and theoretical aspects of the topic.[57]

An alternative pathway through the OM is that taken by several antimicrobial peptides (AMPs) which are capable of disrupting and penetrating through the lipid matrix of the OM.[58] These molecules are typically amphiphilic and polycationic compounds capable of binding to and destabilising anionic lipid interfaces,[59] thus promoting their own penetration through the Gram-negative cell envelope.[60] The LPS-destabilising properties of polycationic AMPs, such as polymyxins, has inspired the design of new synthetic antibiotic candidates which could lead to much needed novel antibacterial compounds capable of overcoming the OM permeability barrier.[61,62] LPS remodelling is a well-known strategy adopted by many Gram-negative organisms that renders the OM more resistant to the effects of several cationic AMPs.[25] Positively charged aminoarabinose or phosphorylethanolamine residues, attached to the phosphate groups of lipid A, reduce the net negative charge on LPS and therefore

the electrostatic binding of AMPs. Although these modifications reduce both the sensitivity towards AMPs and the need for divalent cations for OM stability, in several cases they have also been shown to be costly for bacterial fitness,[63–65] indicating a delicate balance between LPS structure and OM stability.

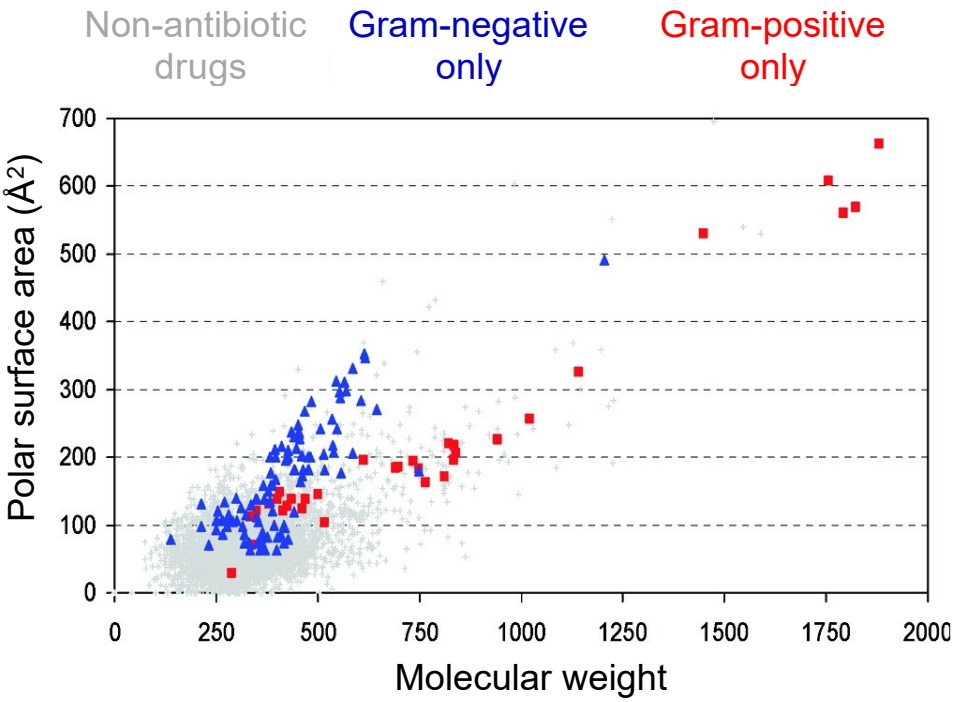

Figure 4: Effect of the OM permeability barrier on the physico-chemical properties of antibacterial compounds. Antibiotics active against Gram-negative bacteria are, on average, smaller and more hydrophilic than drugs active against Gram-positives. The impermeability of the LPS layer restricts penetration across the OM primarily through the water-filled channels of porins which have a cut-off size around 700 Da. Adapted from Ref. 5.

2.4 Structural features of protein-LPS complexes

The interaction between LPS molecules and both membrane and soluble proteins is at the basis of the OM structural stability as well as the several recognition processes that involve LPS. The following two sections are dedicated to summarising some of the aspects of the interactions of LPS with both OM proteins and exogenous proteins involved in recognition processes.

2.4.1 LPS interactions with OM proteins

The crystallographic structures of two OM proteins, the OmpE36 homotrimeric porin[43] (Figure 5a) and the monomeric siderophore FhuA,[66] have been characterized in complex with bound LPS molecules, providing insight on the molecular details of their interaction with LPS in the OM. Analysis of the electron density of the *E. coli* siderophore FhuA revealed the presence of a single LPS molecule bound to the transmembrane protein domain, with the six acyl chains of lipid A adjacent to the hydrophobic external interface of the β-barrel structure.[66] The polar interactions are dominated by six basic residues (i.e. arginines and lysines) present on the protein which form salt bridges and hydrogen bonds with the hydroxyl groups of the inner core OS of LPS, whilst only a few noncharged residues of FhuA take part in the interaction. The crystal structure of the OmpE36 trimer from *Enterobacter cloacae*, which shares a high sequence similarity with the *E. coli* major porin OmpF, contains four LPS molecules per protein trimer in two different binding sites.[43] Three LPS molecules are bound in the cleft between adjacent β-barrel monomers and one LPS molecule on the side of one of the three barrels. In the latter binding site, a Ca^{2+} atom mediates the association of the Kdo residue of LPS with polar amino acids of OmpE36 (Figure 5a), supporting the notion of the importance of divalent cations in stabilising the interaction between LPS and porins, in addition to the well-known LPS-LPS cross-linking in the OM. In contrast, no metal ions were present in the crystal structure of LPS bound to FhuA, where significantly fewer interactions were found between the protein and the Kdo residue of LPS which was found to point away from the protein interface.[66] Furthermore, whilst LPS interacts mainly with basic amino acid side chains in the FhuA complex, the OmpE36 structure indicates a more predominant role of a network of specific hydrogen bonds and polar interactions between the porin and the functional groups of LPS.[43]

In many Gram-negative bacteria the OM is surrounded by a surface layer (S-layer), a protective paracrystalline sheet of proteins anchored to the bacterial envelope through the carbohydrate head group of LPS. The interaction between Rsa, a S-layer protein of *Caulobacter*

crescentus, and the O-antigen of its LPS has been recently elucidated by cryo-EM, which revealed a Ca^{2+} mediated interaction between the protein and the O-PS composed of alternating mannose and N-Acetyl-perosamine residues.[44] As mentioned above in this section, LPS interacts with its transport proteins after being flipped to the periplasmic side of the IM by MsbA, an ATP-binding cassette transporter[28,67] (Figure 5b). The LPS molecule is transferred from the inner to the outer membrane by seven membrane proteins (LptA to LptG), whose complexes have been characterized by cryo-EM[31,68] (Figure 5c) and crystallography.[32] These studies have revealed for the *E. coli* transport system that LPS interacts with a specific pocket at the interface of LptC and LptA.[69]

2.4.2 LPS interactions with exogenous proteins

Due to its unique structure and localisation on the surface of Gram-negative organisms, LPS represents the target of several proteins capable of recognizing and binding different parts of its molecular structure, making it a key player in several recognition processes.[10] Bacterial soluble lectins involved in host recognition and in biofilm formation bind to the heptose of the inner core OS of LPS via Ca^{2+}-bridging between the hydroxyl groups of the monosaccharide residues and the protein surface. [45] Bacteriophages are also known to use LPS as receptors for their tail-spike proteins which they use to bind specifically to the O-antigen of several enterobacteria. Several structures of bacteriophage-LPS complexes have been solved, revealing an elongated binding site formed by a deformed β-helix.[70] LPS also functions as a target for bacterial toxins such as colicin N, and several pyocins. Colicin N recognises and binds specific heptose and hexose cabohydrate residues of the core OS of *E. coli* [36] whilst pyocins interact with the common polysaccharide antigen, a homopolymer of d-rhamnose that forms one of the O-PS chains type found in *P. aeruginosa*.[71]

LPS, whose strong ability to elicit immune responses earned it the name endotoxin, is recognised by several protein receptors in animal and plant hosts, produced by both the adaptive and innate immune system.[4,10] Only a limited number of structures of antibody-glycan com-

plexes are available, mostly Fab fragments of antibody complexed with oligosaccharides of O-antigens from *Salmonella*,[72] *Vibrio cholerae* [73] and *Shigella flexneri* ,[74] or with the Kdo oligosaccharides of the inner core for the *Chlamydiaceae* family.[75] Soluble and membrane-bound mammalian lectins are known to act as pattern recognition receptors for microbial glycoconjugates and several members of this family of proteins have been shown to recognise the sugars present on LPS.[76] The heptose residues of the inner core OS were also found to be the binding site recognised by the surfactant protein-D (SP-D) present in lung mucus, a C-type lectin, characterised by the presence of Ca^{2+} in the carbohydrate binding site.[46,47] Belonging to another class of animal lectins involved in innate immunity, Omentin-1 has been crystallized in complex with D-glycero-D-talo-oct-2-ulosonic acid (KO)[77] a sugar that can substitute one of the two Kdo residues in some Gram-negative species.[78] In contrast macrophage galactose-type lectins (MGL) preferentially bind to the hexose sugars of the outer core OS.[79]

In the activation of the toll-like receptor (TLR) pathway, LPS is first extracted from aggregates by the lipid-binding protein (LBP), then transferred to the cluster of differentiation 14 (CD14) protein. The CD14 protein promotes the formation of a hexameric complex of two copies of LPS, TLR4 and myeloid differentiation factor 2 (MD-2) $(TLR4/MD\text{-}2/LPS)_2$ [11,80] (Figure 5d). LPS alkyl chains are inserted within the hydrophobic pocket of MD-2, and the sugar/phosphate residues stick out and interact with the TLR4 protein, triggering the complex dimerisation. Activation of the TLR4 receptor, and the consequent inflammatory signal cascade, is highly dependent on the acylation pattern and phosphorylation degree of LPS. The degree of occupancy of the MD-2 hydrophobic pocket, dictated by the acylation state of LPS, affects the proximity of the phosphate groups to the TLR4 protein (Figure 5d inset) and therefore the ability of LPS to promote the multimerisation of TLR4/MD-2 complexes and the consequent inflammatory signal cascade.[80] As a result of the structural requirements for signal transduction, hexa-acylated and bi-phosphorylated lipid A represents the most potent agonist of the TLR4 pathway.[11]

Overall, from an analysis of the protein-LPS complexes described, a remarkable diversity of molecular interactions emerges, both in terms of the specific regions of LPS involved as well as the nature of the forces at play. Interactions underlying recognition processes such as those involving lectins, bacteriophages and bacterial toxins, like colicin N and pyocins, primarily target the carbohydrate structures present in the core OS and O-antigen regions, which are significantly more accessible than the buried hydrophobic lipid A. The lipid A moiety plays however a determining role in the recognition by the TLR4-mediated pathway and the subsequent activation of the inflammatory cascade, one of the central processes in host-pathogen interactions involving Gram-negative bacteria. Even the two structures of LPS bound to β-barrel OM proteins available, although both involving broadly the same lipid A and inner core OS regions, highlight significant differences, with a more prominent role of electrostatic interactions in the case of FhuA and a stronger reliance on hydrogen bonding and Ca2+ mediated interactions for OmpE36. As our understanding of the structure of the OM grows, the importance of the interplay between LPS and OM proteins becomes ever more central and deepening our knowledge of these interactions at a molecular level remains of primary importance to fully elucidate the properties of the OM of primary importance to fully elucidate the properties of the OM

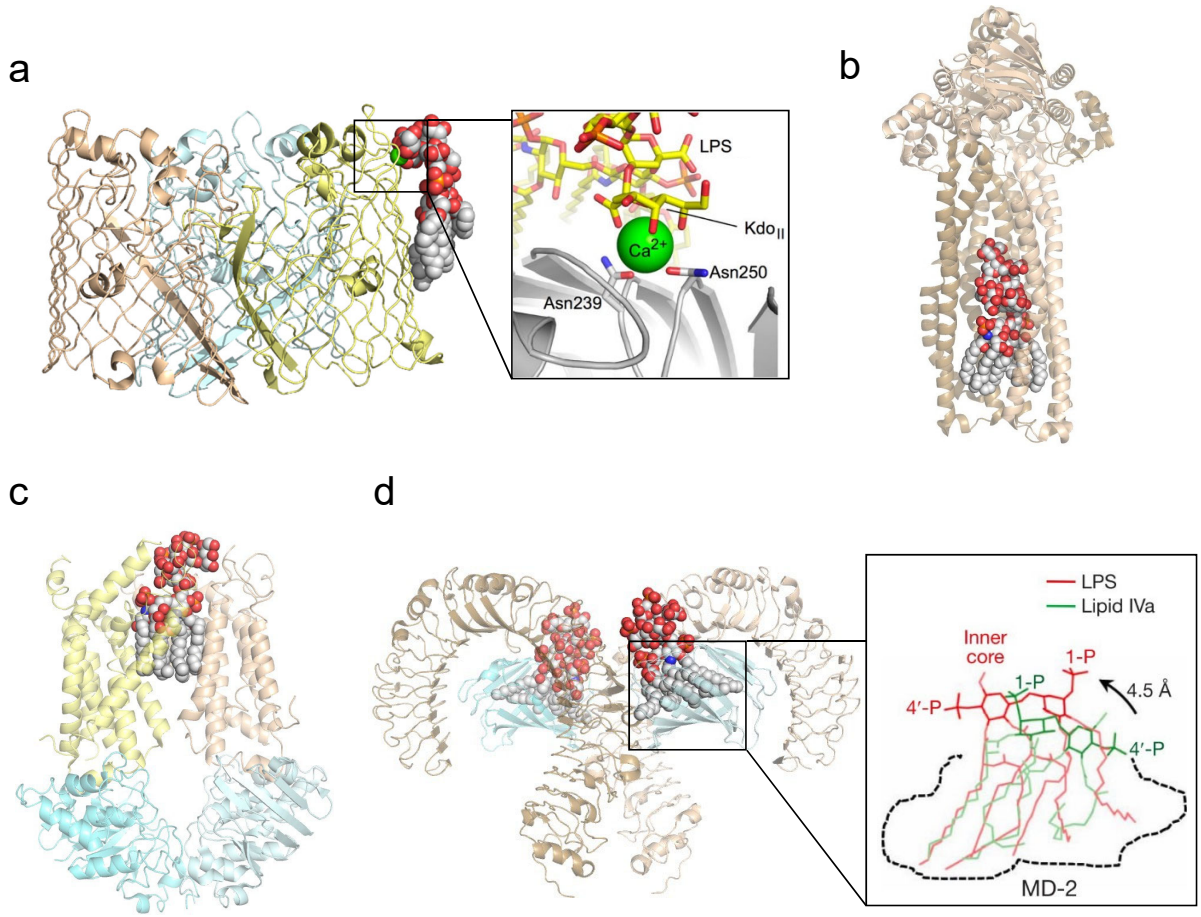

Figure 5: Structures of LPS in complex with different proteins available in the Protein Data Bank. **a)** OmpE36 porin (PDB: 5FVN), showing only one of the LPS molecules present in the structure for clarity. The inset shows the calcium ion binding site mediating the porin-LPS interaction by bridging two asparagine residues with the KDO moiety of LPS, reproduced from Ref. 43 **b)** MsbA transport protein (PDB: 6BPP); **c)** LptB2FG complex transport system (PDB: 6S8H) LptF, LptG and the two LptB molecules are coloured in wheat, yellow and cyan, respectively; **d)** TLR4-MD-2 dimeric complex (PDB: 3FXI) TLR-4 and MD-2 are coloured in wheat and cyan, respectively. The inset shows the different spatial orientations of the phosphate groups of hexa-acylated lipid A (red) and tetra-acylated lipid A (green), respectively a potent agonist and antagonist of the TLR4 pathway, resulting from the different degree of occupancy of the MD-2 pocket (dashed line) by the acyl chains, reproduced from Ref. 80. Proteins are represented by helices, LPS by spheres. Graphics have been prepared using PyMol (Schrödinger).

3 Studies of LPS reconstituted at interfaces

Whilst crystallography and cryo-EM are powerful tools to investigate the structure of individual LPS molecules bound to proteins, the requirements for crystalline and frozen specimens, respectively, preclude their use in studying the structural properties of LPS under conditions comparable to those faced physiologically by bacteria. This has led to the development of a range of *in vitro* models of the OM created by reconstituting layers of different LPS chemotypes, from lipid A to rough mutants to smooth LPS, on planar surfaces to investigate the properties of the lipid matrix of the OM and the interactions with antimicrobial molecules. Compared to the native bacterial surface, *in vitro* OM models are significantly less complex systems which enable the investigation of both structural and biophysical properties of membranes containing LPS. Furthermore, OM models provide a complementary way to study the interactions of antimicrobials with a simplified mimic of the bacterial cell envelope which has been shown to be a powerful approach for the characterisation of the effects of clinically relevant antibiotics at a molecular level, as discussed in the dedicated sections of this review.

Biophysical methods to study OM models. Macroscopic, planar LPS layers are particularly suited for methods based on X-ray[81] and neutron scattering,[82,83] techniques that have provided a detailed description of the structure of LPS reconstituted at both air/liquid and solid/liquid interfaces. Specular reflection techniques, such as X-ray reflectometry (XRR) and neutron reflectometry (NR), are routinely used to probe the elemental composition of molecularly thin films along the direction perpendicular to the plane of the interface with sub-nanometer resolution,[84] which provide information on the thickness and composition of the individual regions of molecules at the interface. Both XRR and NR have been used extensively to study model membranes containing LPS, each approach presenting specific advantages and drawbacks: X-rays can be produced with very high intensity at synchrotron beam lines, enabling fast data acquisition and access to off-specular scattering, such as graz-

ing incidence X-ray diffraction (GIXD), as well as X-ray fluorescence measurements.[85] On the other hand, the unique isotopic sensitivity of neutrons, which differentiate hydrogen from its isotope deuterium, allows exploitation of the so-called isotopic contrast variation, used to highlight specific molecular components within the model membranes.[86–88] The higher penetration depth of neutrons through solid substrates such as silicon crystals, has made them widespread for studies at buried solid/liquid interfaces, whilst X-rays have been used to a larger extent to study LPS monolayers at the air/water interface. In the latter case, access to GIXD measurements provides information on the in-plane ordering and packing parameters of LPS molecules such as the area per hydrocarbon chain, the average size of the ordered domains and the tilt angle of the acyl chains.[89]

In addition to the structural information provided by X-rays and neutron scattering techniques, a range of surface sensitive and biophysical methods have contributed to the characterisation of the properties of LPS at interfaces and their interactions with antimicrobials, complementing the structural information obtained from scattering experiments. These include X-ray fluorescence, [85,90,91] fluorescence microscopy,[92,93] infrared spectroscopy,[94,95] atomic force microscopy (AFM),[92,96,97] surface plasmon resonance (SPR),[94] quartz crystal microbalance with dissipation monitoring (QCM-D),[93,98,99] interfacial rheometry[100] and impedance spectroscopy.[101,102]

In the following sections we review the work done on the structural characterisation of LPS reconstituted in mono- and bilayers, focusing first on Langmuir monolayers at the air/liquid interface to then move on to the studies performed on LPS-containing membranes reconstituted at solid interfaces. Related approaches that remain outside the scope of this review include diffraction studies on LPS multilayers[103–106] and LPS reconstituted into Montal-Muller membranes at the liquid/liquid interface. [92,107,108]

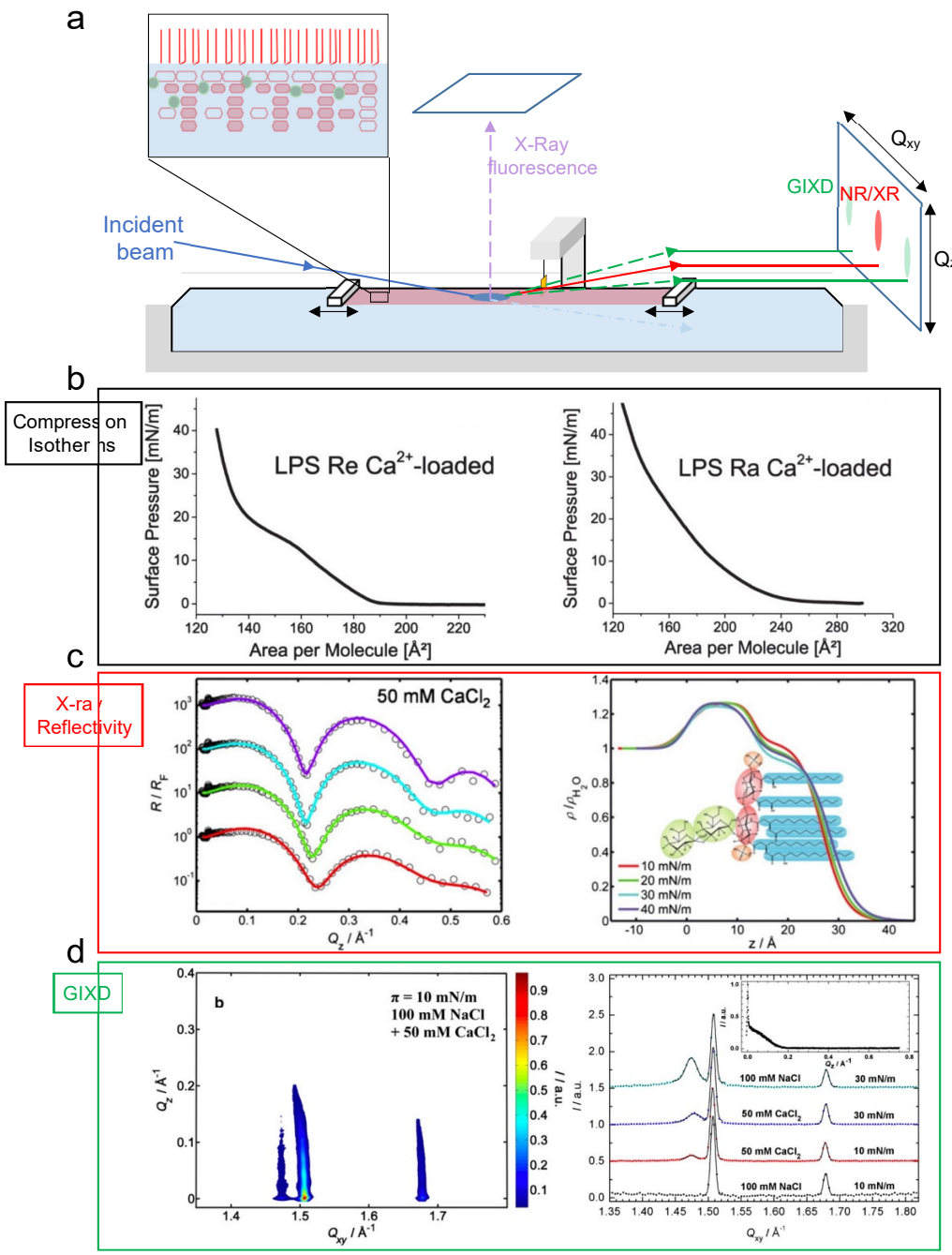

Figure 6: **a)** Schematic representation of the experimental set up used to perform experiments on LPS Langmuir monolayers. In orange the Whilhelmy plate used to measure changes in surface pressure upon compression of the monolayer performed by the movable barriers. The incident beam represents either neutrons or x-rays used in the different experimental techniques **b)** Pressure-area compression isotherm of ReLPS (left) and RaLPS (right) on a subphase containing of 50 mM $CaCl_2$. Reproduced from Ref. 100. **c)** XRR curves (left) and corresponding electron density profiles (right) of a monolayer of ReLPS measured at different surface pressures on a subphase containing 50 mM calcium chloride. **d)** GIXD detector image (left) and integrated signal (right) from ReLPS measured under different subphase and surface pressure conditions. **c)** and **d)** reproduced from Ref. 109.

3.1 LPS monolayers at the air/water interface

A single layer of LPS molecules spread on the water surface of a Langmuir trough is arguably the simplest *in vitro* model of the outer leaflet of the OM. Langmuir monolayers are versatile systems for the biophysical characterisation of lipid layers as they provide control over the the degree of packing of lipid molecules as well as environmental physico-chemical parameters such as temperature, pH and ionic strength.[110] Furthermore, antimicrobial compounds can be introduced in the aqueous subphase below the monolayer to investigate their effects on LPS and gain insights into the interaction at a molecular level. [59,111] Insoluble Langmuir monolayers are also the starting point for the assembly of Langmuir-Blodgett and Langmuir-Schaefer[112] LPS interfaces, reviewed below in the dedicated section, as well as free standing asymmetric bilayers at the liquid/liquid interface, also known as Montal-Muller membranes.[92,107,108]

3.1.1 Surface pressure-area isotherms of LPS

Molecular monolayers are prepared by spreading a solution of LPS in organic solvents onto a clean buffered aqueous subphase, where the monolayer can be compressed using the movable barriers of the trough whilst the surface pressure (which is a measure of the decrease in the interfacial surface tension) is monitored using a Wilhelmy plate (Figure 6a). The measurement yields a compression isotherm, which correlates the change in the surface pressure to the mean molecular area of LPS in the monolayer, providing a tool to sample the isothermal phases of the monolayer as it undergoes compression. Typical lipid packing densities found in biological membranes and estimated to correspond to values of surface pressure between 30 and 35 mN/m for phospholipid membranes,[113,114] can therefore be reproduced in compressed monolayers for biophysical studies. Due to the significant differences in the hydrophilic/hydrophobic balance of different LPS variants, mixtures of organic solvents of different polarity are used to solubilise the various chemotypes prior to their deposition. Lipid A and ReLPS are typically solubilised in mixtures of chloroform and methanol, while

for the more polar LPS with longer carbohydrate headgroups (e.g. RaLPS and smooth LPS), a mixture of phenol, chloroform, and petroleum ether (PCP) 2:5:8 v:v:v is commonly employed.[100,115,116]

Although formation of mixed LPS-phospholipid monolayers had been reported in 1970[117] the first systematic study on Langmuir monolayers of pure lipid A and rough LPS chemotypes was published in 1984 by Brandenburg and Seydel who combined surface pressure measurements with bulk differential thermal analysis and fluorescence spectroscopy to study the phase behaviour of LPS from *S. minnesota*.[115] Isotherms of lipid A monolayers exhibited the plateau typical of the coexistence of the liquid-expanded and the liquid-condensed states, indicating a clear change of phase from a disordered to an ordered state upon compression of the monolayer. The calorimetric and fluorescence measurements identified a well-defined thermotropic phase transition from the gel to the fluid phase, within the temperature range of 40°C - 46°C for lipid A, and 30°C - 37°C for various LPS mutants of increasing core OS size, a trend confirmed in a follow up study by the same group.[118] Even if a clear thermotropic phase transition was measured for all LPS types by calorimetry and fluorescence, the authors noted that the isotherm plateau gradually disappeared as the size of the oligosaccharide region increased, as later reported by several studies on rough LPS and lipid A monolayers from *Escherichia coli* [119–121] and *Salmonella* species[100,122] (Figure 6b). Taken together these observations suggest that as the core OS size increases, the intermolecular interactions in the monolayer become dominated by the bulky headgroup of LPS which overshadow the transition from the liquid expanded to the liquid condensed phase of the acyl chains in the isotherms. This behaviour can be compared to what is observed in the isotherms of gangliosides glycolipids, where the plateau becomes less evident as the size of the carbohydrate head group increases.[123] Indeed, infrared measurements revealed that the acyl chains of ReLPS become ordered as monolayers are compressed to smaller areas even when a plateau is not clearly visible.[95]

Interfacial rheometry measurements have shown how the interactions between the larger core

OS of RaLPS significantly alter the mechanical properties of LPS monolayers when compared to the shorter ReLPS. Whilst monolayers of ReLPS form viscoelastic two-dimensional gels only in the presence of cross-linking divalent cations, RaLPS monolayers display viscoelastic behaviour both in the presence and absence of Ca^{2+} ions upon compression, indicating a stronger interaction between the larger core OS regions.[100] Examining the effects of divalent cations on LPS isotherms has provided useful insights on the biological role of Ca^{2+} and Mg^{2+} for the stability of the OM. Divalent cations have a significant condensing effect on LPS monolayers, reducing the mean molecular area of LPS by means of bridging the repulsive electrostatic interaction arising from its anionic functional groups. This is evident in the isotherms of ReLPS,[100,120] RaLPS[91,94,100,122] and smooth LPS,[116] all of which display, at a given surface pressure, a significant decrease in the mean molecular area in the presence of 50 mM Ca^{2+} (Figure 6b). Interestingly, the condensing effect of divalent cations becomes significantly less evident when isotherms are performed at 10°C.[109] This can be interpreted as a consequence of the higher order favored by the lower kinetic energy in the monolayer at 10°C compared to room temperature, which partially reduces the thermal motion of LPS acyl chains in the monolayer. This in turns promotes tighter packing of LPS molecules thereby reducing the extent to which LPS can be further condensed by divalent cations in the subphase at a given surface pressure.

Grazing incidence X-ray fluorescence (GIXF) measurements have shown how Ca^{2+} completely replaces monovalent K^{+} ions in the core OS region when added to the subphase of the monolayers, indicating a much higher affinity of divalent cations for both Ra[91] and ReLPS[85] compared to monovalent ones. In the presence of divalent cations, the melting temperature of ReLPS raises from 32°C to 36°C and 39°C for Mg^{2+} and Ca^{2+} respectively,[124] an effect reflected in ReLPS isotherms in which the presence of Ca^{2+} lowers the pressure required for the onset of the plateau[100,120] which is in agreement with an increase in the lipids melting temperature.

3.1.2 Vertical structure of LPS monolayers

Specular reflection techniques such as XRR and NR, have provided precise information on the vertical structure (i.e. perpendicular to the plane of the interface) of LPS monolayers. Whilst X-rays are sensitive to the electron density in the sample, neutrons are scattered by the atomic nuclei, thereby providing complementary information on the different regions of the monolayer.[19,116] In reflectometry experiments, a beam of either X-rays or neutrons hits a planar interfacial sample (e.g. a monolayer at the air/water interface) and the reflected intensity is measured, at the same angle of incidence, as a function of the wave vector transfer (Q_z), a combination of incident angle (θ) and wavelength (λ) of the impinging radiation ($Q_z = 4\pi \sin(\theta)\, \lambda^{-1}$).[125] The resulting intensity versus Q_z plot is converted into a profile of the distribution of scattering centers along the perpendicular to the interface versus distance, typically by fitting the data to the reflectivity calculated from a slab model of the interface which describes chemically distinct regions of the sample[19,87,91,126] (Figure 6c). An alternative approach consists in using partial structure factors[127] which account for the independent contributions of each individual region of the monolayer to the overall reflectivity.[116,128]

Rough LPS mutants. A two layers structure, composed of a water-embedded layer corresponding to the GlcN and Kdo head groups and an adjacent air-exposed layer for the acyl chains, is typically used to model reflectivity data from lipid A [121,129,130] and ReLPS.[109,120] For rough LPS with longer core OS such as RcLPS and RaLPS, this minimal two-layer model can be extended to a set of three layers by splitting the carbohydrate head group into an inner core region and an outer core region,[19,131–133] reflecting the different chemical and physical properties of the inner and outer core OS. In particular, the presence of phosphate groups in the inner core, which also drives the accumulation of divalent cations,[91] imparts a higher electron density compared to the outer core which can be measured by XRR.[19,131,132] Although most structural studies have focused primarily on lipid A and rough mutant LPS,

recently the monolayer structure of smooth LPS from *E. coli* serotype O55:B5 has been resolved by a combination of XRR and NR at the air/water interface.[116] Due to the polydisperse nature of the O-PS chains, these are not suitable to be approximated to a single layer of homogeneous density but can be instead described by a stretched exponential function that reflects the decay in O-PS density as a function of distance from the interface.[128]

In addition to the number of sugars present in the core OS and O-PS, the surface pressure and the ionic compositions of the sub-phase affect the overall vertical structureand thickness of LPS monolayers. A comprehensive study on ReLPS by Jeworrek *et al.* systematically addressed the influence of both parameters on the monolayers structure[109] (Figure 6c). The thickness of ReLPS acyl chains was found to change from 13.5 Å to 15.9 Å when compressing monolayers from 10 to 40 mN/m regardless of the specific ionic composition of the subphase, which was instead shown to affect the thickness of the head group region. Specifically, at low compression levels (10 mN/m) the GlcN and Kdo head group of ReLPS was found to be 9.5 Å and 13.3 Å in the presence of Na^+ and Ca^{2+} respectively, indicating a more upright orientation of the Kdo moieties driven by divalent cations mediated cross-linking. For a comparison, lipid A monolayers, which lack the Kdo residues, as expected, display a significantly thinner head group, measuring 3.7 Å , 5.1 Å and 6.2 Å at 10 mN/m, 20 mN/m and 30 mN/m respectively.[121,129] Combining XRR and NR Le Brun *et al.* have addressed the characterisation of monolayers of RcLPS, which contains in its core OS the complete heptose inner region plus two hexose sugars of the outer core OS.[19] Whilst at low surface pressure (10 mN/m) the water-embedded head group layer resembled a single 14 Å thick homogeneous layer, above 20 mN/m an inner and an outer region became clearly distinguishable both by XRR and NR as RcLPS molecules adopt an upright orientation in the compressed monolayer. The inner core is characterised by a higher electron density, measured by X-rays, and a lower volume fraction of water hydrating the inner carbohydrate region, revealed by neutrons, as compared to a more hydrated and less electron dense outer core region. The full core oligosaccharide sequence present in RaLPS reaches an extension of

28 Å to 30 Å with a lipid A region comparable to the other LPS species measuring between 10 Å and 13 Å, depending on the conditions of surface pressure and divalent cations present in the subphase.[90,91,122,131]

Smooth LPS. Recently, the structure of the O-PS at the air/water interface was elucidated by characterising Langmuir monolayers of smooth LPS from *E. coli*.[116] The structural study described a bimodal saccharide distribution across the interface for LPS carrying uncharged O-PS, with a dense core oligosaccharide region followed by an extended and diluted polysaccharide domain. The O-PS "brush" formed by the polydisperse O-side chains, present in a fraction of the LPS molecules, was found to have a maximum extension of 150 Å and 163 Å in the presence and absence of Ca^{2+} respectively. The O-PS conformation was well described within the self-consistent field (SCF) theory adapted for grafted brushes of flexible polymers which was used to estimate the extension of the uncharged O-antigen chains. The theoretical modelling estimated the maximum extension of the O-PS chain to be 160 Å, in close agreement with the values obtained from the reflectivity data analysis.[116]

3.1.3 Lateral structure of LPS monolayers

Whilst specular reflectometry measurements enable access to the vertical structure of LPS monolayers, GIXD provides information on the in-plane lateral arrangement and conformation of LPS molecules within the monolayer.[81,89] Although chain-saturated glycolipids can display two-dimensional ordering of both the lipid acyl chains and the carbohydrate headgroups,[134] no LPS chemotype has been shown to display ordering of the core OS region in GIXD experiments on monolayers. Several studies have instead measured the crystalline arrangement of the acyl chains of lipid A[121,129,130] ReLPS,[109,120] RcLPS[19,132,133] and RaLPS[131] monolayers (Table 1). In GIXD experiments the number of Bragg peaks observed in the diffraction signal along the Q_{xy} direction (Figure 6d) is indicative of the type of packing that

the acyl chains adopt within the monolayer: typically, a single peak indicates ideal hexagonal packing, two peaks arise from a distorted hexagonal configuration (equivalent to centered rectangular) whilst three Bragg peaks indicate an oblique hexagonal packing. [89] Furthermore, the positioning of the peaks in the Q_z direction contains information on the tilting of the acyl chains with respect to the interface plane.

Although complicated by differences in bacterial strains, subphase composition, surface pressure and temperature conditions used for GIXD experiments on monolayers, a comparison of the results available in the literature highlights a certain degree of variablity in the diffraction measurements of LPS monolayers. Even for lipid A molecules from *E. coli* F583 on the same subphase and under the same conditions of surface pressure (30 mN/m), both hexagonal[129] and distorted hexagonal[121] packing have been reported. ReLPS was shown to adopt hexagonal packing and diffract at 20 mN/m only in the presence of added Ca^{2+} ions, whereas a surface pressure of 30 mN/m was required to reproduce the single diffraction peak in the absence of added divalent cations.[120] Another extensive GIXD study on ReLPS monolayers reported instead diffraction corresponding to distorted hexagonal packing even at low (10 mN/m) surface pressures without added calcium ions, however in this case measurements were performed at 10°C which promotes ordering of the lipids.[109] In this study, increasing the pressure above 20 mN/m or adding Ca^{2+} resulted in the splitting of the signal into three peaks indicating the onset of oblique hexagonal packing of the acyl chains of ReLPS (Figure 6d). Unexpectedly, the presence of Ca^{2+} and higher surface pressures resulted in the systematic reduction of the crystalline domains size which was attributed to a higher occurrence of defects in the monolayer, promoted by an increased rigidity of the LPS layer under these conditions.[109] A different study on *E. coli* RcLPS reported an oblique hexagonal packing with the presence of additional molecular tilting of the acyl chains which decreased from 29° to 15° as the monolayer was compressed from 3 to 45 mN/m, in agreement with the increase in thickness measured by XRR and NR.[19] Two separate studies on a different RcLPS chemotype from *S. enterica* showed a single diffraction peak at 20 mN/m indicating

ideal hexagonal packing[132,133] in contrast with the oblique hexagonal arrangement of *E. coli* RcLPS.[19] Hexagonal packing was also observed for *E. coli* RaLPS at 35 mN/m in the presence of 5 mM Ca^{2+}.[131] The diffraction peak disappeared upon removal of Ca^{2+} by means of the chelating agent EDTA supporting the notion that the bridging effect of divalent cations promotes ordering of the monolayer acyl chain region as observed with ReLPS.[109,120] On the other hand no diffraction was observed for RaLPS from *S. enterica* even in the presence of Ca^{2+}[122] although in this case measurements were performed at 25 mN/m whereas diffraction was observed for *E. coli* RaLPS at 35 mN/m.[131] A strain-dependent behaviour of the different RaLPS types cannot be ruled out and future studies could help explain these differences. Although a range of diffraction patterns have been observed for LPS and lipid A, the measured area per hydrocarbon chain has been consistently shown to be between 18 and 22 $Å^2$ in all cases, with no clear trend dictated by surface pressure conditions or subphase composition.[109] At present, there are no studies on the in-plane structure of pure smooth LPS monolayers. A step in this direction is the study by Michel *et al.* who performed GIXD measurements on monolayers made of a mixture of smooth LPS and ReLPS (3:1 w/w).[135] The recent elucidation of the vertical structure of smooth LPS monolayers[116] could pave the way for studies on the lateral organisation of monolayers made entirely of smooth LPS.

Bacterial Strain	**LPS Chemotype**	**Methods**	**Antimicrobials**	**Reference**
S. enterica minnesota	Lipid A, ReLPS, RdLPS, RcLPS, RbLPS, RaLPS	Isotherms	-	115
P. aeruginosa PAO1 H103	ReLPS	Interfacial tensiometry	Polymixin B and E1, Colymicin M, GramicidinS	136
E. coli F583	Lipid A	Isotherms	Protegrin	119

E. coli F583	Lipid A	Isotherms, Impedance spectroscopy	LL-37	101
S. enterica Minnesota R595	Tetra-acyl lipid A, Lipid A, ReLPS	Isotherms, Epi-fluorescence	Polymixin B†	96
S. typhimurium G30/C21	Mono-phosphoryl lipid A	Isotherms	-	137
E. coli F583	Lipid A	Isotherms, GIXD, XRR	Cathelicidins: LL-37, SMAP-29, D2A22	121
S. enterica Minnesota R595	Lipid A, ReLPS	Isotherms, BAM	Polymyxin B and derivatives	138
P. aeruginosa PAO1 O5	Smooth LPS	Isotherms	-	139
Not specified	Lipid A	Isotherms, GIXD, XRR	Protegrin	130
S. enterica R595	Lipid A, ReLPS	Isotherms, IR	Lactoferrin	95
S. enterica Minnesota	RaLPS	Isotherms, GIXOS, MC simulation	Protamine	122
E. coli F583	Lipid A	Isotherms, GIXD, XRR	Synthetic AMPs: OAK-1, AA-1	129

S. enterica R595	ReLPS	GIXF, MC simulations	-	85
E. coli F515	Lipid A, ReLPS	Isotherms, GIXD, GIXOS, MC simulations	Protamine	120
S. enterica Minnesota R595	ReLPS	Isotherms, XRR, GIXD	-	109
S. enterica Minnesota R90	RaLPS	Isotherms, GIXF, XRR	Protamine, synthetic AMP PEP 19-2.5	91
E. coli J5	RcLPS	NR, XR, GIXD, BAM	-	19
P aeruginosa	Not specified	Interfacial tensiometry	Polymyxin B and synthetic AMP WLBU2	140
S. enterica Typhimurium galE mutant	RcLPS‡	Isotherms, XRR, GIXD	Novobiocin	132
S. enterica Minnesota R595, R60	ReLPS, RaLPS	Isotherms, Interfacial rheometry	Protamine	100
E. coli EH100	RaLPS	Isotherms, GIXD	-	131
S. enterica Minnesota	ReLPS, Smooth LPS	Isotherms, GIXD, BAM	Plasticins	135

E. coli EH100	RaLPS	Isotherms, MD simulations	-	141
E. coli O55:B5	Smooth LPS	Isotherms, NR, XRR	-	116
S. enterica Typhimurium galE mutant	RcLPS‡	Isotherms, GIXD, XRR, MD simulations	LL-37	133
S. enterica Minnesota R60	RaLPS	Isotherms, GIXF, XRR	Benzalkonium chloride, benzyl alcohol	90
E. coli	ReLPS, RdLPS	Isotherms	Ampicillin, Cefsulodin, Ciprofloxacin, Novobiocin, Rifampicin, Azythromicin, Telithromicin, Gentamicin, Polymyxin B, Polymyxin E	142
E. coli J5	RcLPS	Isotherms, NR, IR	Synthetic AMPs: $G(IIKK)_3I\text{-}NH_2$, $C8\text{-}G(IIKK)_2I\text{-}NH_2$	126

Table 1: Studies addressing LPS Langmuir monolayers listed in chronological order of publication. GIXD: grazing incidence x-ray diffraction, XRR: X-ray reflectometry, BAM: brewster angle microscopy, IR infrared spectroscopy, GIXOS: grazing-incidence x-ray out of specular plane scattering, NR neutron reflectometry, GIXF: grazing incidence X-ray fluorescence, MD: molecular dynamics, MC: Monte Carlo (†) Interaction studied after transferring the monolayer onto a solid substrate. (‡) Modified RcLPS obtained from antibiotic resistant and sensitive strains.

3.1.4 Antimicrobial studies at the air/water interface

Lipid monolayers have been used extensively to test antimicrobial interactions with model membranes.[59,111,143] Given the primary role of LPS in the OM as the first line of defence against noxious compounds, numerous studies have addressed the interaction of antimicrobial compounds with LPS and lipid A monolayers (Table 1). Typically, after compressing the monolayer at surface pressures between 20 and 30 mN/m, antimicrobial compounds are injected into the aqueous subphase and their insertion in the monolayer is assessed by monitoring changes in surface pressure at a constant monolayer area or, conversely, by observing the changes in the area required to maintain a constant surface pressure. Once the system reaches equilibrium, NR, XRR and GIXD measurements can be used to probe the structural changes in the monolayer and assess the effects of the interaction.

Antimicrobial peptides (AMPs) are one of the most studied categories of compounds in this context as they represent a class of membrane active compounds with potential for development of antimicrobials less susceptible to antibiotic resistance.[59,144] The first comprehensive study of the effects of AMPs on LPS monolayers was published by Zhang *et al.* who used interfacial tensiometry to measure the interaction of three polymyxins (i.e. polymyxin B, polymyxin E1 and colimycin M) and gramicidin S with ReLPS monolayers.[136] These antibiotics are cyclic cationic AMPs approved for clinical use to treat Gram-negative infections topically and the study addressed their ability to insert into monolayers made of ReLPS compared to phospholipid monolayers, mimicking the outer and cytoplasmic membrane, respectively. Interfacial tensiometry experiments use a simpler version of a Langmuir trough

that lacks the movable barrier, where lipids are added to the surface until a desired surface pressure is achieved, in this case 18 mN/m. This approach simplifies the measurements by eliminating the step of performing the compression isotherm but allows for a greater number of experiments to be performed. The study elegantly correlated the ability of the AMPs to insert into the different types of lipid monolayers with cell killing and cell permeabilisation assays to provide a comprehensive picture of the diverse mechanisms of action of these antibiotics.[136]

Structural studies on LPS-AMP interactions: XRR and GIXD Neville *et al.* performed the first structural studies on lipid A monolayers, using XRR and GIXD to investigate the effects of two natural cathelicidin AMPs, LL-37 and SMAP-29, and the synthetic analogue D2A22. [121] In the study, monolayer experiments were performed on a conventional Langmuir trough and the results showed how the ability of the AMPs to insert in the monolayer is heavily influenced by the concentration of antimicrobials and the surface pressure conditions. Overall, AMP insertion was shown to be directly proportional to the AMP concentration in the subphase (higher penetration at 0.1 μg/ml compared to 0.04 μg/ml) and inversely proportional to the surface pressure applied during the interaction (lower penetration at 40 mN/m compared to 30 mN/m). Although insertion isotherms revealed a significant amount of AMPs penetrating into the lipid A monolayer, GIXD data only showed minor effects on the lateral ordering of lipid A which preserved an unperturbed distorted hexagonal packing after AMPs addition. XRR indicated a moderate change in thickness and electron density of the monolayer induced by the interaction with LL-37 which was mainly localised in the head group region of lipid A. A significantly stronger effect of LL-37 was reported in a later study on RcLPS monolayers by Martynowycz *et al.*, who compared the interaction of LL-37 with LPS isolated from two strains of *S. enterica*, one of which expresses LPS modified with the addition of an extra acyl chain and an amino arabinose residue that increase resistance towards the AMP.[133] XRR and GIXD indicated a much more prominent alteration of

the monolayer structure by LL-37 compared to what observed in the work of Neville *et al.* on lipid A,[101] with a prominent loss of lateral ordering in the monolayers as well as significant differences in the vertical structure before and after interaction with the AMP. LPS modifications from the drug-resistant bacteria were shown to reduce antibiotic penetration in the monolayer, providing molecular-level insights into the mechanisms of antibiotic resistance by combining biophysical techniques with results from molecular dynamic simulations. In a previous study, Nobre *et al.* combined XRR and GIXD to show how the same modifications were effective in preventing penetration of the small molecule antibiotic novobiocin through monolayers of LPS extracted from sensitive and resistant strains of *S. enterica*.[132] Contrary to what was observed with LL-37, however, novobiocin caused an unexpected increase in the lateral ordering of LPS monolayers as revealed by the enhanced intensity of the diffraction peak measured by GIXD after the interaction. The peculiar order-inducing effects of novobiocin remain unusual when compared to the loss of order caused by the majority of antimicrobial compounds studied by GIXD, suggesting a rather different mechanism of action of this antibiotic. Complete loss of lateral ordering was also reported for antimicrobials such as protamine[120] and the synthetic biomimetic AMPs OAK-1 and AA-1[129] whilst protegrin was shown to only partially affect the two dimensional order of lipid A monolayers.[130]

Effect of divalent cations Several studies have focused on the role of divalent cations in reducing the susceptibility of LPS monolayers towards the penetration of antimicrobials as in the case of protamine,[100,120,122] synthetic peptides[91] and cationic surfactants.[90] In all cases the presence of mM quantitites of Ca^{2+} ions in the aqueous subphase significantly reduced the susceptibility of LPS monolayers to penetration of antimicrobials. In this context, the use of GIXF has provided depth-resolved information on the ion distribution profiles of monovalent (K^+) and divalent (Ca^{2+}) cations[85] complementary to the structural information on the LPS-antimicrobial interaction obtained by XRR.[90,91]

Structural studies on LPS-AMP interactions: NR Although limited by the requirement for deuterium-labelled LPS, which is not commercially available and is extracted from bacteria grown in heavy water,[86] NR has also been recently employed to study the interaction between RcLPS monolayers and synthetic AMPs.[126] An alternative NR approach that circumvents the purification of deuterated LPS is that proposed by Bello *et al.* who used mixed monolayers of commercially available LPS and deuterium labelled-phospholipids to investigate the effects of lactoferrin and LL-37.[145] If on the one hand this approach has the advantage of enhancing the neutron scattering signal from the mixed monolayer, on the other, the presence of a significant amount of intercalated phospholipids does not reproduce the natural conditions of the OM, increasing antimicrobial compounds accessibility to the monolayer's hydrophobic region. The use of NR to elucidate the kinetics of AMP interactions with Langmuir monolayers has been shown to be a promising approach thanks to the fast acquisition times at low incident angles on deuterated monolayers..[111] Collection times are currently around four minutes per measurement, but the sampling time is set to decrease as instruments are upgraded, opening the possibility of monitoring real-time structural changes produced by AMP interactions with LPS monolayers.

3.2 LPS at solid interfaces

Along with LPS monolayers at the air/water interface, *in vitro* OM models assembled onto solid surfaces have provided a range of useful platforms to study the structure and properties of thin films containing LPS. Immobilisation of LPS onto solid interfaces has been mainly tackled using two approaches: (i) self-assembly of either LPS suspensions[94,146] or mixed phospholipid/LPS vesicles[93,98,99,102] or (ii) Langmuir-Blodgett (LB) and Langmuir-Schaefer (LS) transfer of monolayers from the air/water interface[94,128,131,147–149] (Figure 7). Self-assembly methods, such as vesicle fusion, are based on relatively straight-forward protocols and have the advantage of in-situ sample preparation, which enables real-time monitoring of lipid adsorption processes onto the solid substrates. In addition, bilayer formation by fusion of OM

vesicles, secreted and purified from bacterial cultures, is an approach that has been used to create *in vitro* OM models that closely reproduce the protein and lipid composition found in the OM.[98,99] Although a certain degree of lipid asymmetry between the inner and outer bilayer leaflets can be achieved via self-assembly, in part facilitated by the large excluded volume of the bulky LPS head group, typically, sequential LB/LS transfer of phospholipids and LPS layers afford a higher level of control on lipid asymmetry and composition of the individual bilayer leaflets but require a more complex sample preparation.[94,148]

Solid-supported bilayers (SLBs) are versatile model membranes which can be probed by a wide range of biophysical methods and have been used extensively for membrane biophysics studies.[150] Compared to Langmuir monolayers, SLBs enable the formation of more complex model membranes that can recreate both leaflets of the lipid bilayer, providing a complementary platform for the study of reconstituted biological membranes. Some biophysical methods employed for Langmuir monolayers, such as NR, XRR or infrared spectroscopy, are also applicable to the study of SLBs, whilst techniques like GIXD and GIXF find their main application at the air/water interface. On the other hand, SLBs can be probed by additional surface-sensitive techniques such as surface plasmon resonance (SPR),[94] quartz crystal microbalance with dissipation (QCM-D), [93,98,99] atomic force microscopy (AFM)[92,93,97] and impedance spectroscopy.[102]

3.2.1 Self-assembled LPS layers

Self-assembled LPS monolayers Both rough[94] and smooth LPS[146] have been shown to self-assemble into monolayers when deposited from aqueous suspensions onto silica substrates coated with a hydrophobic layer of octadecyltrichlorosilane (OTS) (Figure 8a). *P. aeruginosa* smooth LPS monolayers, bearing an O-PS containing anionic O-antigen repeating units, were characterised by XRR to investigate the extension and conformation of the O-PS and the effects of divalent cations on its structure.[146] The study showed that in the presence of mM quantities of divalent cations the charged polysaccharide chains of the O-PS collapse to a

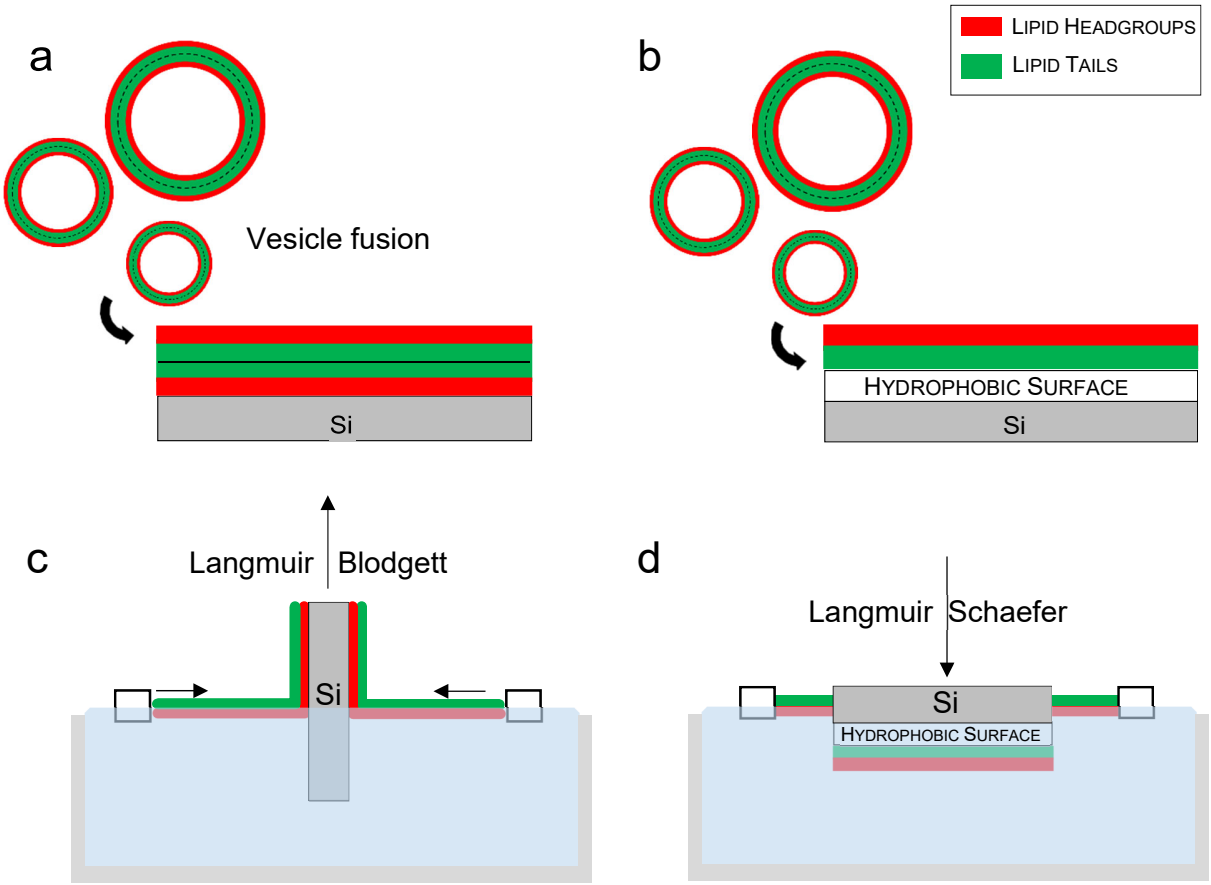

Figure 7: Schematic representation of methods for the preparation of monolayers and bilayers containing LPS onto solid substrates. In the cartoon the solid substrate is represented by a silicon wafer which is commonly used as support to form model membranes providing a hydrophilic surface that can also be functionalised and rendered hydrophobic by coating it with alkyl-silanes such as OTS. **a**) Fusion of vesicles onto a hydrophilic and **b**) hydrophobic substrate, yielding a lipid bilayer or a monolayer respectively. **c**) Langmuir-Blodgett and **d**) Langmuir-Schaefer transfer of a lipid monolayer from the air/liquid interface onto a solid substrate. In **d**, the hydrophobic surface can be either a chemically grafted alkyl-silane layer, producing a solid-supported LPS monolayer, or the hydrophobic face of a phospholipid monolayer previously transferred using the LB method yielding an asymmetric phopsholipid/LPS bilayer. See figure 8 for a schematic representation of the resulting OM models obtained.

more compact and dense layer indicating a strong condensation effect of calcium ions on the O-PS conformation. In another study, monolayers of RaLPS assembled onto OTS-coated silica substrates were investigated to probe the interaction between the model bacterial surface and the AMP polymyxin B.[94] In this case, the use of deuterium-labelled OTS, coupled with the isotopic sensitivity of neutrons, enabled resolution of the individual structures

of the alkyl-silane layer and the LPS acyl chains investigated by NR. The formation of the monolayer of RaLPS was additionally monitored by SPR and infrared spectroscopy providing complementary information on the self-assembly process of LPS monolayers onto hydrophobic surfaces.

Self-assembled bilayers containing LPS Mixed liposomes containing phospholipids and LPS (either rough LPS from *E. coli* or smooth LPS from *S. typhimurium*) were shown to assemble into LPS-containing bilayers on silica surfaces with an LPS content of up to 50%$_w$ in the case of rough LPS, or 20%$_w$ for the smooth type[93](Figure 8b). By monitoring the adsorption process via QCM-D, Kaufmann *et al.* showed how the presence of divalent cations is required to facilitate bilayer formation, which is considerably slower or ultimately hindered in the absence of added calcium ions. The binding of lectins to different types of LPS incorporated in the mixed bilayers was investigated in the same study using fluorescence microscopy, demonstrating how a specific LPS could not only be incorporated but remained fully accessible to binding by lectins. In another study, vesicles made exclusively of RdLPS were reported to form lipid bilayers on mica surfaces yielding bilayers with a coverage of 86% of the hydrophilic surface as measured by AFM.[97] This value increased to 92% when the mica was functionalized with a positively charged polyethyleneimine layer. The study also investigated the formation of RaLPS bilayers by vesicle fusion, concluding that lower coverage and more irregularities are associated with bilayers formed from LPS with larger oligosaccharide cores. These observations, together with the results described above from Kaufmann and co-workers,[93] support the notion that larger carbohydrate headgroups can hinder the formation of LPS bilayers by interfering with the adhesion forces required for vesicle fusion. Whilst hydrophobic interactions drive the lipid self-assembly onto hydrophobic surfaces, bilayer formation onto a hydrophilic surface is highly sensitive to the charge balance between vesicles and the substrate, with a crucial role played by divalent cations and LPS head group size.

RcLPS has been reconstituted via vesicle fusion into high-coverage tethered lipid bilayers both in its pure form as well as mixed with phospholipids.[102] Anderson *et al.* used a gold-coated silicon surface to exploit gold-thiol chemistry and create a tethered monolayer that provided the substrate for the formation of the RcLPS layer. The tethering leaflet was formed by a thiolipid, analogue of diphytanoyl-glycero-phosphocholine (DPhyPC) modified with a tethering segment containing the thiol anchor; the distal bilayer leaflet consisted of RcLPS either in its pure form or mixed with a small amount of DPhyPC (2-6 $\%_{wt}$). The resulting tethered membranes were then structurally characterised using NR. The in-plane density of the tethering monolayer was shown by impedance spectroscopy measurements to play a critical role in the stabilisation of LPS against treatment with EDTA, with higher tethers densities providing higher stability when divalent cations were removed from the model membranes. A similar stabilising effect was observed when vesicle fusion was performed with mixtures of RcLPS and low amounts of phospholipids, suggesting a possible reduction of the overall negative charge and steric hindrance of LPS headgroups by the intercalated phospholipids. [102]

Self-assembled bilayers containing LPS and OM proteins One of the advantages of using surfaces modified by grafted tethering layers or polymer cushions is the additional space left between the membrane and the solid substrate which can facilitate the incorporation of transmembrane proteins.[151,152] An example of a protein-containing solid-supported OM model is that developed by Hsia *et al.* who used OM vesicles secreted by a deep rough *E. coli* mutant to create bilayers via self-assembly with a composition resembling that of the native OM (Figure 8c). Using fluorescence spectroscopy and QCM-D, the study showed that, although OM vesicles do not spontaneously form a bilayer upon adsorption onto hydrophilic silicon substrates, SLB formation can be induced by the addition of PEGylated lipids to the adsorbed intact OM vesicles, inducing formation of a planar bilayer.[98] Furthermore,

using OM vesicles containing fluorescently labelled OM proteins and a proteinase K-based assay, the native protein orientation was shown to be largely retained after SLB formation, suggesting that the approach preserves a significant degree of membrane asymmetry. More recently, the same group used the aforementioned approach to create SLBs using OM vesicles secreted by clinically relevant isolates of *P. aeruginosa*, *E. cloacae* and *A. baumannii* which express smooth LPS, and used the OM models to investigate interactions with antibiotics (Figure 8c).[99]

3.2.2 Langmuir-Blodgett and Langmuir-Schaefer LPS layers

Langmuir-Blodgett (LB) and Langmuir-Schaefer (LS) monolayer transfer techniques represent an alternative method to self-assembly processes that have been used to create solid-supported OM models. In contrast to the in-situ preparation of SLBs afforded by self-assembly, OM models prepared by LB and LS depositions require a more complex preparation as well as a specialised Langmuir trough for transferring the monolayers from the air/water interface onto the solid substrates[88] (Figure 7). A significant advantage provided by LB and LS assembly approaches is the substantial control provided by the layer-by-layer deposition on the lipid composition and packing of each individual leaflet which enables formation of high-coverage fully asymmetric bilayers that mimic the distribution of lipids in the OM.

Although LB/LS approaches enable the construction of complex interfacial structures, these methods have not yet been used to incorporate OM proteins in reconstituted OM models that contain LPS. An inherent challenge of embedding OM proteins in model membranes using this approach is that the layer-by-layer assembly implies that proteins must remain stable at the air-water interface, as well as in a planar monolayer with only half their transmembrane domain embedded in a hydrophobic environment, at least until the second lipid layer is formed. It has been shown that the porin OmpF can be incorporated into dipalmitoylphosphoglycerol (DPPG) monolayers at the air/water interface by rupturing proteoliposomes

on the water surface which formed a stable lipid monolayer containing one of the major porins found in *E. coli*.[153] A different approach involves solubilising lipids and proteins in organic solvent prior to monolayer deposition, which has been shown to be applicable to some membrane proteins such as those found in myelin.[154]

Phospholipids/LPS asymmetric bilayers Using LB and LS depositions to stack an inner leaflet of deuterium-labelled phospholipids and an outer layer of hydrogenous LPS, the group of Lakey and co-workers has studied extensively the structural and functional aspects of a range of asymmetric OM models using NR. In this context, the differential sensitivity of neutrons towards hydrogen and deuterium enables the quantification and monitoring of lipid asymmetry whilst providing information on the structure of the OM models along the perpendicular to the interface. Isotopically asymmetric bilayers consisted of an inner leaflet of tail-deuterated dipalmitoylphosphocholine (d_{62}DPPC) deposited via LB transfer (Figure 7c) followed by a layer of rough LPS deposited via LS deposition (Figure 7d) to yield an asymmetric OM model. This approach has been used to create asymmetric bilayers containing different chemotypes of rough LPS both directly onto silicon[94,131,147,148] (Figure 8e) as well as onto gold surfaces functionalised with a monolayer of ω-thio-phospholipids, which yield asymmetric bilayers floating over a 2 nm water reservoir separating the bilayer and the substrate[149] (Figure 8f). The applications of isotopically asymmetric bilayers are not limited to structural studies by NR but extend to other isotope-sensitive techniques such as infrared spectroscopy. Specifically, attenuated total reflection infrared (ATR-IR) spectroscopy, which distinguishes between carbon-hydrogen and carbon-deuterium bond vibrations, has been shown capable of probing the individual lipid phase transitions of the inner and outer leaflets of asymmetric d_{62}DPPC/RaLPS OM model bilayers.[94] Both solid-supported and floating d_{62}DPPC/LPS bilayers retain high levels of lipid asymmetry in the presence of mM levels of Ca^{2+}, but are significantly destabilised by the addition of EDTA which depletes the aqueous solution of divalent cations.[131,149] Removal of Ca^{2+} causes a

significant reduction of asymmetry as a result of interleaflet lipid mixing and an increased interfacial roughness caused by the enhanced electrostatic repulsion of the anionic LPS in the absence of charge-bridging divalent cations.

Inverse LPS/LPS bilayers Rodriguez-Loureiro *et al.* used LB and LS methods to deposit onto an OTS-coated silicon surface two layers of smooth LPS oriented with the respective carbohydrate regions facing each other to mimic the interface between neighbouring interacting Gram-negative bacteria found in colonies and biofilms (Figure 8d).[128] Once assembled, the distance between the two LPS interfaces was tuned by varying the relative humidity, which in turn generates a dehydration pressure that controls the thickness of the water layer sandwiched between the LPS layers, producing a separation of the surfaces that varies between 90 Å and 330 Å. Structural characterisation of the system was performed using ellipsometry and NR, providing a detailed and comprehensive structural characterisation of smooth LPS layers and their interacting O-PS domains. The pressure-distance relation was well-described by the model of Alexander and de Gennes typically applied to model uncharged flexible polymer brushes at interfaces. The same study also addressed the effect of the depletion of Ca^{2+} ions on a single solid-supported smooth LPS monolayer which induced the formation of monolayer defects that caused water penetration in the hydrophobic region of the monolayer.[128]

3.2.3 Antimicrobial studies at the solid/liquid interface

A number of studies have exploited solid-supported OM models to investigate the interactions of antimicrobials with LPS and model Gram-negative bacterial surfaces. In particular, due to their high affinity for LPS, a significant fraction of these studies focused on antibiotics of the polymyxin family of compounds on self-assembled[94,98,99,102] and LB/LS-based OM models.[94,155,156] The group of Daniel and co-workers used QCM-D and fluorescence microscopy to quantify the amount of polymyxin B binding to OM models assembled via fusion

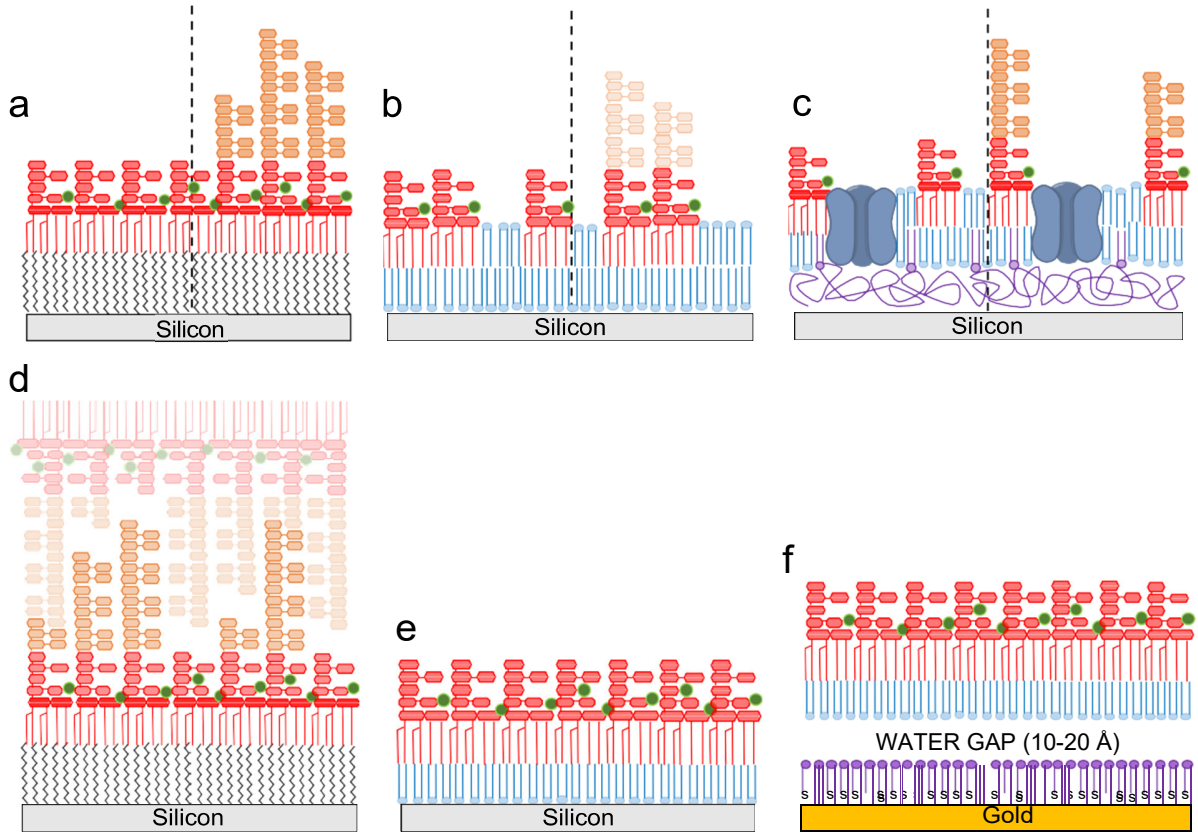

Figure 8: Schematic representation of several solid supported OM models created by self-assembly (**a**, **b** and **c**) or by using LB/LS deposition techniques (**d**, **e** and **f**) with the respective references that describe their characterisation. **a)** LPS monolayer adsorbed onto a chemically grafted hydrophobic monolayer of alkyl-silane (in black) containing Ra (left) (Ref. 94) and smooth LPS (right) (Ref. 146). RaLPS is shown in red and the OPS in orange, in green divalent cations **b)** Mixed LPS/phospholipid solid supported bilayer containing rough (left) or smooth (right) LPS (Ref. 93). Phospholipids are shown in blue **c)** Solid supported bilayer reconstituted using OM vesicels containing OM proteins and rough (left) (Ref. 98) or smooth LPS (right) (Ref. 99). PEGylated phospholipids are shown in purple **d)** Interacting smooth LPS monolayers deposited onto alkyl-silane monolayer (Ref. 128). **e)** Asymmetric bilayer containing phospholipids in the inner leaflet and rough LPS in the outer leaflet (Ref. 94,126,131,147,148,155,156). **f)** Asymmetric bilayer containing phospholipids in the inner leaflet and RaLPS in the outer leaflet floating onto a grafted monolayer of *ω*-thio-phosphocholine (purple) (Ref. 149).

of OM vesicles isolated from deep-rough[98] and smooth strains,[99] which provided insights into the extent of antimicrobial binding as well as alterations of visco-elastic properties of these protein-containing OM models. Andersson *et al.* showed how higher densities of the tether used to provide the substrate for the self-assembly of RcLPS had a stabilising effects against

the disruptive action of polymyxin E (also known as colistin).[102] A comparison between the interaction of polymyxin B with self-assemmbled RaLPS monolayers and asymmetric d_{62}DPPC/RaLPS LB/LS bilayers can be found in a recent study that combined NR, SPR and ATR-IR spectroscopy.[94] The different approaches used to assemble OM models were shown to have a significant effect on the outcome of the measured interaction. Polymyxin B was shown to bind in a concentration-dependent manner to self-assembled RaLPS monolayers in the gel phase (i.e. at room temperature) within a physiologically relevant concentration range. On the other hand, asymmetric d_{62}DPPC/RaLPS bilayers prepared via LB/LS depositions remained unaffected by a concentration 10 times higher under the same temperature conditions. Only after heating the d_{62}DPPC/RaLPS asymmetric membrane through the RaLPS phase transition, with a mid-point at 36°C measured by infrared spectroscopy, the disruptive effects of the antibiotic on the membrane structure became apparent, reproducing the temperature-dependent bactericidal effects observed for polymyxin B on *E. coli*[157] and providing evidence supporting the relevance of a phase transition of LPS to a liquid crystalline state in the OM at physiological temperatures.

Han *et al.* used asymmetric d_{62}DPPC/lipid A bilayers to compare the effects of polymyxin B to those of its synthetic analogue octapeptin A3.[155] When compared to other polymyxins, octapeptin A3 displayed an enhanced ability to penetrate into the OM model bilayers, reaching the phospholipid inner leaflet. The enhanced membrane penetration measured *in vitro* was found to correlate with its higher bactericidal activity measured against the *P. aeruginosa* strains which were used to extract the lipid A reconstituted in in the model OM. In a later study, the same group addressesd the effects of *P. aeruginosa* lipid A modifications, specifically de-acylation and addition of positively charged aminosugars to the GlcN, on the interaction with polymyxin B and two of its synthetic analogues.[156] By comparing the structural data obtained by NR on the penetration of the AMPs in the OM models with the biological effects on bacterial viability and gene regualtion, they were able to show that polymyxin B-induced lipid A deacylation plays a significant role in high-level resistance of

P. aeruginosa. Recently, the effects of two synthetic cationic AMPs, designed to bind and disrupt LPS membranes, were tested using d_{62}DPPC/RcLPS asymmetric bilayers by Gong *et al* .[126] The study provided a comprehensive structural characterisation of the effects of the synthetic AMPs by combining NR measurements on both Langmuir monolayers and asymmetric bilayers with small angle scattering and nuclear magnetic resonance data. The differences in the overall positive charge and the hydrophobicity of the two AMPs tested translated into significantly different disruptive effects on the model membranes. In particular, combining data on the AMP interactions with isotopically asymmetric d_{62}DPPC/RcLPS and with fully deuterated d_{62}DPPC/dRcLPS provided a detailed structural description of the mechanisms through which the AMPs interact with and disrupt the OM. In a comparative study of the interaction between the antimicrobial protein colicin N and asymmetric bilayers made of either d_{62}DPPC/RaLPS or d_{62}DPPC/RdLPS, Clifton *et al.* showed how the presence of the additional uncharged oligosaccharide in the outer core of RaLPS significantly reduced both the amount of bound atimicrobial and the strength of the LPS-colicin N electrostatic interaction.[148] Furthermore, due to the oblate shape of the colicin N protein, NR measurements provided a clear picture of the orientation of the membrane-bound protein which was shown to interact with the LPS surface of the OM models by adsorbing with its major axis parallel to the membrane surface.

3.3 Simulation studies

As discussed in the previous sections, much of our knowledge about the structure and conformation of LPS interfaces is based on surface scattering techniques, such as reflectometry and x-ray fluorescence, which lend themselves to integration with complementary computer simulations.[158] Early computer models of LPS molecules date back to the 1990s. In a combined experimental/simulation study by Kastowsky et al., an ensemble of molecular conformations was predicted with the help of Monte Carlo simulations employing empirical conformation energies, however ignoring partial atomic charges.[159] Roughly a decade later the conforma-

tion of O-side chains was addressed by Pink and coworkers with coarse-grained Monte Carlo (CGMC) simulations.[160] For this purpose, each monosaccharide was represented by an either charged or uncharged sphere, water was treated implicitly as a dielectric medium, but ions were treated explicitly as charged particles. The simulations predicted that divalent cations could render the polysaccharide "brush" impenetrable to certain antimicrobial peptides. The CGMC approach has later been used for the interpretation of experimental results on LPS monolayers described earlier.[85,120,122,146] Around the same time the first force-field-based atomistic molecular dynamics (MD) simulations of LPS surfaces were carried out.[161] The trajectories with a 1 ns duration on a surface accommodating 4 x 4 LPS molecules suggested that Ca^{2+} ions interacting with inner core phosphate groups exhibit a well defined structural arrangement. With the increase in computational performance, MD simulations on LPS surfaces have become more widespread,[162–166] and the force fields were validated and optimized with respect to experimental observables, such as area per molecule, L_β to L_α phase transition, and orientation order parameter.[163,167] More recently, a coarse-grained force field has been parametrized within the MARTINI framework in order to make large systems and long time scales accessible to quantitative modeling. [168]

Very recently, the OM of *Pseudomonas aeruginosa*, a bacterial species well known for antibiotic resistance, was studied by all-atom and coarse-grained simulations.[169] The structural properties of the layer were reproduced and compared with phospholipid bilayers. The simulations revealed that a removal of divalent cations induces the rupture of the LPS/phospholipid bilayer, with the consequent exposure of negatively charged groups, and a phase transition from lamellar to inverted cubic arrangements. A more complete overview of molecular simulations of Gram-negative bacterial membranes is given in a recent review article by Im & Khalid.[170]

The use of MD simulations has also been extended to include OM proteins in the computational models which have been used to investigate aspects of the interaction between porins and LPS.[171–173] A current limitation in the molecular simulation of LPS surfaces is

that conventional simulation methods do not account for the variable protonation state of the ionisable groups, although their pKa-values depend on various parameters like packing density and ion concentrations, as can be determined experimentally, for example by total-reflection x-ray fluorescence. [85,174] In the future, this limitation may be overcome by the implementation of constant-pH simulation schemes.[175] Finally, a promising emerging application of MD simulations is the use of computational models for the interpretation of reflectivity data which provides practical physico-chemical constraints when decoding the data obtained with techniques such as NR.[176]

4 Conclusions and outlook

Advancing our understanding of the properties of the Gram-negative OM is one of the key steps in the fight against the growing antibiotic resistance of pathogens belonging to this category. The various OM models reviewed here serve as versatile tools for the investigation of structural and functional properties of the Gram-negative bacterial surface as well as providing a range of valuable platforms to study the effects of antimicrobial compounds at a molecular level. Whilst the greatly reduced complexity of an OM model significantly facilitates structural studies, it also poses the question of how closely reconstituted LPS layers can mimic the natural bacterial cell envelope. In the context of antimicrobial interactions, several studies have combined the detailed physico-chemical characterisation enabled by the adoption of OM models with assays on bacterial viability, cell permeability and alteration of gene expression, thereby correlating data obtained on membrane models with experiments on living organisms. Such approaches validate and contextualise biophysical data obtained on *in vitro* models with the behaviour of the natural system. Studies on modified LPS that confers resistance to antimicrobials, whereby LPS extracted from resistant organisms is reconstituted in OM models to study the mechanisms of antibiotic resistance at a molecular level, are a primary example of this approach.[132,133,155,156]

Increasing the complexity of reconstituted LPS interfaces, for example by exploiting the self-assembly of OM vesicles containing native lipids and proteins, represents a strategy that opens up several possibilities for the development of screening platforms to study antimicrobial binding.[98,99] These approaches sensibly increase the number and diversity of biomolecules found on the bacterial surface that can be studied as targets for antimicrobial binding. Furthermore these methods hold potential for high throughput drug-screening applications that could emerge from combining optical, mechanical or electrical measurements in biosensors[177] with standardised fabrication strategies for the preparation of SLB arrays.[178] For structural studies, higher complexity can represent a drawback, especially for reflectometry techniques, which can offer sub-nanometer resolution but rely on a reduced complexity of the system, which is required for modelling the data during the analysis. LPS Langmuir monolayers represent the simplest case and X-ray techniques, such as XRR, GIXD and GIXF, have been used extensively in this context (Table 1). The structure of LPS at the solid/liquid interface, on the other hand, is better suited to be studied by neutrons which can, not only penetrate easily through solid substrates and reach buried interfaces, but, due to their isotopic sensitivity, provide additional contrast to resolve structural features such as membrane asymmetry[131,147,149] and antibiotic penetration[94,126,148] which are difficult to characterise with other approaches.[83]

Given the different types of techniques applicable to air/liquid and solid/liquid interfaces the choice of a particular type of OM model ultimately comes down to the scientific problem in object and the type of biophysical technique required to elucidate it. For questions regarding in-plane ordering and ion distribution, Langmuir monolayers provide the ideal platform for GIXD and GIXF studies. On the other hand, quantitative information on antimicrobial binding can be more accurately extracted from solid-supported OM models using techniques such as QCMD and SPR. If the main focus is instead on the overall bilayer structure, as in the case of studies of lipid asymmetry or OM-proteins incorporation, then solid-supported OM model bilayers provide the most suitable platforms. An aspect that

should always be kept in mind, however, is that the complementary use of different biophysical methods is the most reliable approach for a comprehensive understanding of the properties of biologi- cal interfaces. Combining experiments on multiple types of interfaces can provide precious complementary pieces of information that taken together yield a more complete picture of the process under investigation.

So far reconstitution studies have addressed predominantly LPS from *E. coli* and *Salmonella* species, focusing primarily on lipid A and rough LPS. Nonetheless, the development of the models and methods reviewed here can be readily adapted to study other bacterial species, opening up possibilities for the characterisation of diverse types of LPS,[3,4] with a particular focus on wild-type smooth LPS. Together with the development of experimental techniques, the refinement of computer simulation packages is expected to provide an ever more realistic *in silico* OM model.[170] Advances in the modeling of complex asymmetric phospholipid:LPS bilayers, which can also include embedded porins, have made significant steps forward in recent years and will continue to provide important complementary information to the experimental data. The analysis of scattering data in particular is an area where simulations and experiments could merge their contribution to provide clear molecular-level descriptions of LPS layers and model bacterial surfaces.[176]

Acknowledgements

NP acknowledges support from Nordforsk - Nordic Neutron Science Program (Grant 106881) and wishes to thank Prof. Jeremy Lakey for insightful feedback on the manuscript. SM and ES thank the German Federal Ministry of Research and Education (BMBF) within the Röntgen-Ångström cluster (Grant 05K16ECA). AI acknowledges support from Glyco@Alps (ANR-15-IDEX-02) and Labex Arcane/CBH-EUR-GS (ANR-17-EURE-0003).

References

(1) Nikaido, H. Molecular Basis of Bacterial Outer Membrane Permeability Revisited. *Microbiol. Mol. Biol. Rev.* **2003**, *67*, 593–656.

(2) Henderson, J. C.; Zimmerman, S. M.; Crofts, A. A.; Boll, J. M.; Kuhns, L. G.; Herrera, C. M.; Trent, M. S. The Power of Asymmetry: Architecture and Assembly of the Gram-Negative Outer Membrane Lipid Bilayer. *Annu. Rev. Microbiol.* **2016**, *70*, 255–278.

(3) Di Lorenzo, F.; Duda, K. A.; Lanzetta, R.; Silipo, A.; De Castro, C.; Molinaro, A. A Journey from Structure to Function of Bacterial Lipopolysaccharides. *Chemical Reviews* **2021**,

(4) Molinaro, A.; Holst, O.; Lorenzo, F. D.; Callaghan, M.; Nurisso, A.; D'Errico, G.; Zamyatina, A.; Peri, F.; Berisio, R.; Jerala, R.; Jiménez-Barbero, J.; Silipo, A.; Martín-Santamarí, S. Chemistry of lipid a: At the heart of innate immunity. *Chem. - A Eur. J.* **2015**, *21*, 500–519.

(5) O'Shea, R.; Moser, H. E. Physicochemical Properties of Antibacterial Compounds : Implications for Drug Discovery Perspecti V e Physicochemical Properties of Antibacterial Compounds : Implications for Drug Discovery. **2008**, *51* .

(6) Tommasi, R.; Brown, D. G.; Walkup, G. K.; Manchester, J. I.; Miller, A. A. ESKAPEing the labyrinth of antibactrial discovery. *Nature Reviews Drug Discovery* **2015**, 529–542.

(7) Zhang, G.; Meredith, T. C.; Kahne, D. On the essentiality of lipopolysaccharide to Gram-negative bacteria. *Current Opinion in Microbiology* **2013**, *16*, 779–785.

(8) Simpson, B. W.; Trent, M. S. Pushing the envelope: LPS modifications and their consequences. *Nature Reviews Microbiology* **2019**, *17*, 403–416.

(9) Raetz, C. R. H.; Whitfield, C. Lipopolysaccharide Endotoxins. *Annu. Rev. Biochem.* **2002**, *71*, 635–700.

(10) Raetz, C. R. H.; Reynolds, C. M.; Trent, M. S.; Bishop, R. E. Lipid A modification systems in Gram-negative bacteria. *Annu Rev Biochem* **2007**, *76*, 295–329.

(11) Bryant, C. E.; Spring, D. R.; Gangloff, M.; Gay, N. J. The molecular basis of the host response to lipopolysaccharide. *Nature reviews. Microbiology* **2010**, *8*, 8–14.

(12) Alexander, C.; Rietschel, E. T. Bacterial lipopolysaccharides and innate immunity. *J. Endotoxin Res.* **2001**, *7*, 167–202.

(13) Heinrichs, D. E.; Yethon, J. A.; Whitfield, C. Molecular basis for structural diversity in the core regions of the lipopolysaccharides of Escherichia coli and Salmonella enterica. *Mol. Microbiol.* **1998**, *30*, 221–232.

(14) Holst, O. The structures of core regions from enterobacterial lipopolysaccharides - An update. *FEMS Microbiol. Lett.* **2007**, *271*, 3–11.

(15) Stenutz, R.; Weintraub, A.; Widmalm, G. The structures of Escherichia coli O-polysaccharide antigens. *FEMS Microbiol. Rev.* **2006**, *30*, 382–403.

(16) Whitfield, C.; Williams, D. M.; Kelly, S. D. Lipopolysaccharide O-antigens-bacterial glycans made to measure. *J. Biol. Chem.* **2020**, *295*, 10593–10609.

(17) Hölzer, S. U.; Schlumberger, M. C.; Jäckel, D.; Hensel, M. Effect of the O- antigen length of lipopolysaccharide on the functions of type III secretion systems in Salmonella enterica. *Infection and Immunity* **2009**, *77*, 5458–5470.

(18) King, J. D.; Kocíncová, D.; Westman, E. L.; Lam, J. S. Lipopolysaccharide biosynthesis in Pseudomonas aeruginosa. *Innate Immunity* **2009**, *15*, 261–312.

(19) Le Brun, A.; Clifton, L.; Halbert, C.; Lin, B.; Meron, M.; Holden, P.; Lakey, J.; Holt, S. Structural Characterization of a Model Gram-Negative Bacterial Surface Us- ing Lipopolysaccharides from Rough Strains of Escherichia coli. *Biomacromolecules* **2013**, *14*, 2014–2022.

(20) Browning, D. F.; Wells, T. J.; França, F. L.; Morris, F. C.; Sevastsyanovich, Y. R.; Bryant, J. A.; Johnson, M. D.; Lund, P. A.; Cunningham, A. F.; Hobman, J. L.; May, R. C.; Webber, M. A.; Henderson, I. R. Laboratory adapted Escherichia coli K-12 becomes a pathogen of Caenorhabditis elegans upon restoration of O antigen biosynthesis. *Molecular Microbiology* **2013**, *87*, 939–950.

(21) Peterson, a. a.; McGroarty, E. J. High molecular weight components in lipopolysaccharides of Salmonella typhmurium, Salmonella minnesota, and Escherichia coli. *J Bact* **1985**, *162*, 738–745.

(22) Hitchcock, P. J.; Leive, L.; Makela, P. H.; Rietschel, E. T.; Morrison, D. C. Lipopolysaccharide Nomenclature-Past , Present , and Futuret. *Journal of Bacteriology* **1986**, *166*, 699–705.

(23) Ruiz, N.; Kahne, D.; Silhavy, T. J. Transport of lipopolysaccharide across the cell envelope: The long road of discovery. *Nat. Rev. Microbiol.* **2009**, *7*, 677–683.

(24) Whitfield, C.; Stephen Trent, M. Biosynthesis and export of bacterial lipopolysaccharides. *Annu. Rev. Biochem.* **2014**, *83*, 99–128.

(25) Needham, B. D.; Trent, M. S. Fortifying the barrier: the impact of lipid A remodelling on bacterial pathogenesis. *Nature Reviews Microbiology* **2013**, *11*, 467–481.

(26) Pagnout, C.; Sohm, B.; Razafitianamaharavo, A.; Caillet, C.; Offroy, M.; Leduc, M.; Gendre, H.; Jomini, S.; Beaussart, A.; Bauda, P.; Duval, J. F. Pleiotropic effects of rfa-gene mutations on Escherichia coli envelope properties. *Scientific Reports* **2019**, *9*, 1–16.

(27) Chang, V.; Chen, L.-y.; Wang, A.; Yuan, X. The Effect of Lipopolysaccharide Core Structure Defects on Transformation Efficiency in Isogenic Escherichia coli BW25113 rfaG , rfaP , and rfaC Mutants. **2010**, *14*, 101–107.

(28) Mi, W.; Li, Y.; Yoon, S. H.; Ernst, R. K.; Walz, T.; Liao, M. Structural basis of MsbA-mediated lipopolysaccharide transport. *Nature* **2017**, *549*, 233–237.

(29) Ruan, X.; Monjarás Feria, J.; Hamad, M.; Valvano, M. A. Escherichia coli and Pseudomonas aeruginosa lipopolysaccharide O-antigen ligases share similar membrane topology and biochemical properties. *Molecular Microbiology* **2018**, *110*, 95–113.

(30) Sherman, D. J.; Xie, R.; Taylor, R. J.; George, A. H.; Okuda, S.; Foster, P. J.; Needleman, D. J.; Kahne, D. Lipopolysaccharide is transported to the cell surface by a membrane-to-membrane protein bridge. *Science* **2018**, *359*, 798–801.

(31) Li, Y.; Orlando, B. J.; Liao, M. Structural basis of lipopolysaccharide extraction by the LptB 2 FGC complex. *Nature* **2019**, *567*, 486–490.

(32) Owens, T. W.; Taylor, R. J.; Pahil, K. S.; Bertani, B. R.; Ruiz, N.; Kruse, A. C.; Kahne, D. Structural basis of unidirectional export of lipopolysaccharide to the cell surface. *Nature* **2019**, *567*, 550–553.

(33) Okuda, S.; Sherman, D. J.; Silhavy, T. J.; Ruiz, N.; Kahne, D. Lipopolysaccharide transport and assembly at the outer membrane: The PEZ model. *Nature Reviews Microbiology* **2016**, *14*, 337–345.

(34) Abellon-Ruiz, J.; Kaptan, S. S.; Basle, A.; Claudi, B.; Bumann, D.; Kleinekathofer, U.; van den Berg, B. Structural basis for maintenance of bacterial outer membrane lipid asymmetry. *Nature microbiology* **2017**, *2*, 1616–1623.

(35) Lundstedt, E.; Kahne, D.; Ruiz, N. Assembly and Maintenance of Lipids at the Bacterial Outer Membrane. *Chemical Reviews* **2021**, *121*, 5098–5123.

(36) Johnson, C. L.; Ridley, H.; Marchetti, R.; Silipo, A.; Griffin, D. C.; Crawford, L.; Bonev, B.; Molinaro, A.; Lakey, J. H. The antibacterial toxin colicin N binds to the inner core of lipopolysaccharide and close to its translocator protein. *Mol. Microbiol.* **2014**, *92*, 440–452.

(37) Plésiat, P.; Nikaido, H. Outer membranes of Gram-negative bacteria are permeable to steroid probes. *Mol. Microbiol.* **1992**, *6*, 1323–1333.

(38) Ghai, I.; Ghai, S. Understanding antibiotic resistance via outer membrane permeability. *Infection and Drug Resistance* **2018**, *11*, 523–530.

(39) Vaara, M. Agents that increase the permeability of the outer membrane. *Microbiol. Rev.* **1992**, *56*, 395–411.

(40) Leive, L. A non specific increase in permeability in escherichia coli produced by EDTA. *Proceedings of the National Academy of Sciences of the United States of America* **1965**, *53*, 745–750.

(41) Leive, L. Studies on the permeability change produced in coliform bacteria by ethylenediaminetetraacetate. *Journal of Biological Chemistry* **1968**, *243*, 2373–2380.

(42) Leive, L.; Shovlin, V. K.; Mergenhagen, S. E. Physical, chemical, and immunological properties of lipopolysaccharide released from Escherichia coli by ethylenediaminetetraacetate. *Journal of Biological Chemistry* **1968**, *243*, 6384–6391.

(43) Arunmanee, W.; Pathania, M.; Solovyova, A. S.; Le Brun, A. P.; Ridley, H.; Baslé, A.; van den Berg, B.; Lakey, J. H. Gram-negative trimeric porins have specific LPS binding sites that are essential for porin biogenesis. *Proceedings of the National Academy of Sciences* **2016**, 201602382.

(44) von Kugelgen, A.; Tang, H.; Hardy, G. G.; Kureisaite-Ciziene, D.; Brun, Y. V.;

Stansfeld, P. J.; Robinson, C. V.; Bharat, T. A. M. In Situ Structure of an Intact Lipopolysaccharide-Bound Bacterial Surface Layer. *Cell* **2020**, *180*, 348–358.

(45) Marchetti, R.; Malinovska, L.; Lameignere, E.; Adamova, L.; de Castro, C.; Cioci, G.; Stanetty, C.; Kosma, P.; Molinaro, A.; Wimmerova, M.; Imberty, A.; Silipo, A. Burkholderia cenocepacia lectin A binding to heptoses from the bacterial lipopolysaccharide. *Glycobiology* **2012**, *22*, 1387–1398.

(46) Wang, H.; Head, J.; Kosma, P.; Brade, H.; Muller-Loennies, S.; Sheikh, S.; McDonald, B.; Smith, K.; Cafarella, T.; Seaton, B.; Crouch, E. Recognition of heptoses and the inner core of bacterial lipopolysaccharides by surfactant protein d. *Biochemistry* **2008**, *47*, 710–720.

(47) Littlejohn, J. R.; da Silva, R. F.; Neale, W. A.; Smallcombe, C. C.; Clark, H. W.; Mackay, R. A.; Watson, A. S.; Madsen, J.; Hood, D. W.; Burns, I.; Greenhough, T. J.; Shrive, A. K. Structural definition of hSP-D recognition of Salmonella enterica LPS inner core oligosaccharides reveals alternative binding modes for the same LPS. *PLoS One* **2018**, *13*, e0199175.

(48) Jarosławski, S.; Duquesne, K.; Sturgis, J. N.; Scheuring, S. High-resolution architecture of the outer membrane of the Gram-negative bacteria Roseobacter denitrificans. *Molecular Microbiology* **2009**, *74*, 1211–1222.

(49) Benn, G.; Mikheyeva, I. V.; Inns, P. G.; Forster, J. C.; Ojkic, N.; Bortolini, C.; Ryadnov, M. G.; Kleanthous, C.; Silhavy, T. J.; Hoogenboom, B. W. Phase separation in the outer membrane of Escherichia coli. *Proceedings of the National Academy of Sciences* **2021**, *118*, e2112237118.

(50) Koebnik, R.; Locher, K. P.; Van Gelder, P. Structure and function of bacterial outer membrane proteins: barrels in a nutshell. *Molecular microbiology* **2000**, *37*, 239–253.

(51) Nikaido, H. Porins and specific channels of bacterial outer membranes. *Mol. Microbiol.* **1992**, *6*, 435–442.

(52) Decad, G. M.; Nikaido, H. Outer membrane of gram negative bacteria. XII. Molecular sieving function of cell wall. *Journal of Bacteriology* **1976**, *128*, 325–336.

(53) Delcour, A. H. Outer Membrane Permeability and Antibiotic Resistance. *Biochim Biophys Acta.* **2009**, *1794*, 808–816.

(54) Zgurskaya, H.; Löpez, C.; Gnanakaran, S. Permeability Barrier of Gram-Negative Cell Envelopes and Approaches to Bypass it. *ACS Infect Dis.* **2015**, *1*, 512–522.

(55) Tommasi, R.; Iyer, R.; Miller, A. A. Antibacterial Drug Discovery: Some Assembly Required. *ACS infectious diseases* **2018**, *4*, 686–695.

(56) Pages, J. M.; James, C. E.; Winterhalter, M. The porin and the permeating antibiotic: a selective diffusion barrier in Gram-negative bacteria. *Nature Reviews Microbiology* **2008**, 893–903.

(57) Prajapati, J. D.; Kleinekathöfer, U.; Winterhalter, M. How to Enter a Bacterium: Bacterial Porins and the Permeation of Antibiotics. *Chemical Reviews* **2021**, *121*, 5158–5192.

(58) Mookherjee, N.; Anderson, M. A.; Haagsman, H. P.; Davidson, D. J. Antimicrobial host defence peptides: functions and clinical potential. *Nature Reviews Drug Discovery* **2020**, *19*, 311–332.

(59) Ciumac, D.; Gong, H.; Hu, X.; Lu, J. R. Membrane targeting cationic antimicrobial peptides. *Journal of Colloid and Interface Science* **2019**, *537*, 163–185.

(60) Hancock, R. E.; Sahl, H. G. Antimicrobial and host-defense peptides as new anti-infective therapeutic strategies. *Nature Biotechnology* **2006**, *24*, 1551–1557.

(61) Alfei, S.; Schito, A. M. Positively charged polymers as promising devices against multidrug resistant gram-negative bacteria: A Review. *Polymers* **2020**, *12* .

(62) Alfei, S.; Schito, A. M. From nanobiotechnology, positively charged biomimetic dendrimers as novel antibacterial agents: A review. *Nanomaterials* **2020**, *10*,1–50.

(63) Yang, Q. et al. Balancing mcr-1 expression and bacterial survival is a delicate equilibrium between essential cellular defence mechanisms. *Nature Communications* **2017**, *8*, 1–12.

(64) Tietgen, M.; Semmler, T.; Riedel-Christ, S.; Kempf, V. A.; Molinaro, A.; Ewers, C.; Göttig, S. Impact of the colistin resistance gene mcr-1 on bacterial fitness. *International Journal of Antimicrobial Agents* **2018**, *51*, 554–561.

(65) Da Silva, G.; Domingues, S. Interplay between Colistin Resistance, Virulence and Fitness in Acinetobacter baumannii. *Antibiotics* **2017**, *6*, 28.

(66) Ferguson, A. D.; Welte, W.; Hofmann, E.; Lindner, B.; Holst, O.; Coulton, J. W.; Diederichs, K. A conserved structural motif for lipopolysaccharide recognition by procaryotic and eucaryotic proteins. *Structure* **2000**, *8*, 585–592.

(67) Ho, H. et al. Structural basis for dual-mode inhibition of the ABC transporter MsbA. *Nature* **2018**, *557*, 196–201.

(68) Tang, X. et al. Cryo-EM structures of lipopolysaccharide transporter LptB2FGC in lipopolysaccharide or AMP-PNP-bound states reveal its transport mechanism. *Nat Commun* **2019**, *10*, 4175.

(69) Laguri, C.; Sperandeo, P.; Pounot, K.; Ayala, I.; Silipo, A.; Bougault, C. M.; Molinaro, A.; Polissi, A.; Simorre, J. P. Interaction of lipopolysaccharides at intermolecular sites of the periplasmic Lpt transport assembly. *Sci Rep* **2017**, *7*, 9715.

(70) Kang, Y.; Gohlke, U.; Engstrom, O.; Hamark, C.; Scheidt, T.; Kunstmann, S.; Heinemann, U.; Widmalm, G.; Santer, M.; Barbirz, S. Bacteriophage Tailspikes and Bacterial O-Antigens as a Model System to Study Weak-Affinity Protein-Polysaccharide Interactions. *J Am Chem Soc* **2016**, *138*,9109–9118.

(71) McCaughey, L. C.; Josts, I.; Grinter, R.; White, P.; Byron, O.; Tucker, N. P.; Matthews, J. M.; Kleanthous, C.; Whitchurch, C. B.; Walker, D. Discovery, charac- terization and in vivo activity of pyocin SD2, a protein antibiotic from Pseudomonas aeruginosa. *Biochemical Journal* **2016**, *473*, 2345–2358.

(72) Cygler, M.; Rose, D. R.; Bundle, D. R. Recognition of a cell-surface oligosaccharide of pathogenic Salmonella by an antibody Fab fragment. *Science* **1991**, *253*, 442–445.

(73) Villeneuve, S.; Souchon, H.; Riottot, M. M.; Mazie, J. C.; Lei, P.; Glaudemans, C. P.; Kovac, P.; Fournier, J. M.; Alzari, P. M. Crystal structure of an anti-carbohydrate antibody directed against Vibrio cholerae O1 in complex with antigen: molecular basis for serotype specificity. *Proc Natl Acad Sci U S A* **2000**, *97*, 8433–8438.

(74) Normand, V.-L.; B., F. A. S.; Phalipon, A.; Belot, F.; Guerreiro, C.; Mulard, L. A.; Bentley, G. A. Structures of synthetic O-antigen fragments from serotype 2a Shigella flexneri in complex with a protective monoclonal antibody. *Proc Natl Acad Sci U S A* **2008**, *105*, 9976–9981.

(75) Haji-Ghassemi, O.; Muller-Loennies, S.; Saldova, R.; Muniyappa, M.; Brade, L.; Rudd, P. M.; Harvey, D. J.; Kosma, P.; Brade, H.; Evans, S. V. Groove-type recognition of chlamydiaceae-specific lipopolysaccharide antigen by a family of antibodies possessing an unusual variable heavy chain N-linked glycan. *J Biol Chem* **2014**, *289*, 16644–16661.

(76) Vasta, G. R.; Ahmed, H.; Tasumi, S.; Odom, E. W.; Saito, K. Biological roles of

lectins in innate immunity: molecular and structural basis for diversity in self/non-self recognition. *Adv Exp Med Biol* **2007**, *598*, 389–406.

(77) McMahon, C. M.; Isabella, C. R.; Windsor, I. W.; Kosma, P.; Raines, R. T.; Kiessling, L. L. Stereoelectronic Effects Impact Glycan Recognition. *J Am Chem Soc* **2020**, *142*, 2386–2395.

(78) Isshiki, Y.; Zähringer, U.; Kawahara, K. Structure of the core-oligosaccharide with a characteristic D-glycero-alpha-D-talo-oct-2-ulosylonate-(2->4)-3-deoxy-D-manno-oct-2- ulosonate [alpha-Ko-(2->4)-Kdo] disaccharide in the lipopolysaccharide from Burkholderia cepacia. *Carbohydrate Research* **2003**, *338*, 2659–2666.

(79) Maalej, M.; Forgione, R. E.; Marchetti, R.; Bulteau, F.; Thepaut, M.; Lanzetta, R.; Laguri, C.; Simorre, J. P.; Fieschi, F.; Molinaro, A.; Silipo, A. Human Macrophage Galactose-Type Lectin (MGL) Recognizes the Outer Core of Escherichia coli Lipooligosaccharide. *Chembiochem* **2019**, *20*, 1778–1782.

(80) Park, B. S.; Song, D. H.; Kim, H. M.; Choi, B. S.; Lee, H.; Lee, J. O. The structural basis of lipopolysaccharide recognition by the TLR4-MD-2 complex. *Nature* **2009**, *458*, 1191–1195.

(81) Stefaniu, C.; Brezesinski, G. X-ray investigation of monolayers formed at the soft air/water interface. *Curr. Opin. Colloid Interface Sci.* **2014**, *19*, 216–227.

(82) Lakey, J. H. Recent advances in neutron reflectivity studies of biological membranes. *Curr. Opin. Colloid Interface Sci.* **2019**, *42*, 33–40.

(83) Paracini, N.; Clifton, L.; Lakey, J. H. Studying the surfaces of bacteria using neutron scattering: finding new openings for antibiotics. *Biochemical Society transactions* **2020**, *48* .

(84) Foglia, F.; Lawrence, M. J.; Barlow, D. J. Studies of model biological and bio-mimetic membrane structure: Reflectivity vs diffraction, a critical comparison. *Current Opinion in Colloid & Interface Science* **2015**, *2*, 1–9.

(85) Schneck, E.; Schubert, T.; Konovalov, O. V.; Quinn, B. E.; Gutsmann, T.; Brandenburg, K.; Oliveira, R. G.; Pink, D. A.; Tanaka, M. Quantitative determination of ion distributions in bacterial lipopolysaccharide membranes by grazing-incidence X-ray fluorescence. *Proc. Natl. Acad. Sci. U. S. A.* **2010**, *107*, 9147–9151.

(86) Le Brun, A. P.; Clifton, L. A.; Holt, S. A.; Holden, P. J.; Lakey, J. H. *Methods Enzymol.*, 1st ed.; Elsevier Inc., 2016; Vol. 566; pp 231–252.

(87) Clifton, L. A.; Neylon, C.; Lakey, J. H. In *Lipid-Protein Interactions: Methods and Protocols*; Kleinschmidt, J. H., Ed.; Humana Press: Totowa, NJ, 2013; pp 119–150.

(88) Clifton, L. A.; Hall, S. C. L.; Mahmoudi, N.; Knowles, T. J.; Heinrich, F.; Lakey, J. H. In *Lipid-Protein Interactions: Methods and Protocols*; Kleinschmidt, J. H., Ed.; Springer New York: New York, NY, 2019; pp 201–251.

(89) Als-Nielsen, J.; Jacquemain, D.; Kj, K.; Leveiller, F.; Lahav, M.; Leiserowitz, L. Principles and applications of grazing incidence X-ray and neutron scattering from ordered molecular monolayers at the air-water interface. *Phys. Reps.* **1994**, *246*, 251–313.

(90) Thoma, J.; Abuillan, W.; Furikado, I.; Habe, T.; Yamamoto, A.; Gierlich, S.; Kaufmann, S.; Brandenburg, K.; Gutsmann, T.; Konovalov, O.; Inoue, S.; Tanaka, M. Specific localisation of ions in bacterial membranes unravels physical mechanism of effective bacteria killing by sanitiser. *Scientific Reports* **2020**, *10*, 1–12.

(91) Abuillan, W.; Schneck, E.; Körner, A.; Brandenburg, K.; Gutsmann, T.; Gill, T.; Vorobiev, A.; Konovalov, O.; Tanaka, M. Physical interactions of fish protamine and

antisepsis peptide drugs with bacterial membranes revealed by combination of specular x-ray reflectivity and grazing-incidence x-ray fluorescence. *Physical Review E - Statistical, Nonlinear, and Soft Matter Physics* **2013**, *88*, 1–11.

(92) Paulowski, L.; Donoghue, A.; Nehls, C.; Groth, S.; Koistinen, M.; Hagge, S. O.; Böhling, A.; Winterhalter, M.; Gutsmann, T. The Beauty of Asymmetric Membranes: Reconstitution of the Outer Membrane of Gram-Negative Bacteria. *Front. Cell Dev. Biol.* **2020**, *8*, 1–14.

(93) Kaufmann, S.; Ilg, K.; Mashaghi, A.; Textor, M.; Priem, B.; Aebi, M.; Reimhult, E. Supported lipopolysaccharide bilayers. *Langmuir* **2012**, *28*, 12199–12208.

(94) Paracini, N.; Clifton, L. A.; Skoda, M. W.; Lakey, J. H. Liquid crystalline bacterial outer membranes are critical for antibiotic susceptibility. *Proc. Natl. Acad. Sci. U. S. A.* **2018**, *115*, E7587–E7594.

(95) Kerth, A.; Garidel, P.; Howe, J.; Alexander, C.; Mach, J.-P.; Waelli, T.; Blume, A.; Rietschel, E.; Brandenburg, K. An Infrared Reflection-Absorption Spectroscopic (IRRAS) Study of the Interaction of Lipid A and Lipopolysaccharide Re with Endotoxin-Binding Proteins. *Medicinal Chemistry* **2009**, *5*, 535–542.

(96) Roes, S.; Seydel, U.; Gutsmann, T. Probing the properties of lipopolysaccharide monolayers and their interaction with the antimicrobial peptide polymyxin B by atomic force microscopy. *Langmuir* **2005**, *21*, 6970–6978.

(97) Tong, J.; McIntosh, T. J. Structure of supported bilayers composed of lipopolysaccharides and bacterial phospholipids: Raft formation and implications for bacterial resistance. *Biophys. J.* **2004**, *86*, 3759–3771.

(98) Hsia, C. Y.; Chen, L.; Singh, R. R.; DeLisa, M. P.; Daniel, S. A Molecularly Complete Planar Bacterial Outer Membrane Platform. *Scientific Reports* **2016**, *6*, 1–14.

(99) Mohamed, Z. J.; Shin, J.-H.; Ghosh, S.; Sharma, A.; Pinnock, F.; Naser, S. F. B. E.; Dörr, T.; Daniel, S. Clinically Relevant Bacteria Outer Membrane Models for Antibiotic Screening Applications. *ACS Infect. Dis. Submitted* **2021**,

(100) Herrmann, M.; Schneck, E.; Gutsmann, T.; Brandenburg, K.; Tanaka, M. Bacterial lipopolysaccharides form physically cross-linked, two-dimensional gels in the presence of divalent cations. *Soft Matter* **2015**, *11*, 6037–6044.

(101) Neville, F.; Cahuzac, M.; Nelson, A.; Gidalevitz, D. The interaction of antimicrobial peptide LL-37 with artificial biomembranes: Epifluorescence and impedance spectroscopy approach. *Journal of Physics Condensed Matter* **2004**, *16* .

(102) Andersson, J.; Fuller, M. A.; Wood, K.; Holt, S. A.; Köper, I. A tethered bilayer lipid membrane that mimics microbial membranes. *Phys. Chem. Chem. Phys.* **2018**, *20*, 12958–12969.

(103) Abraham, T.; Schooling, S. R.; Nieh, M. P.; Kučerka, N.; Beveridge, T. J.; Katsaras, J. Neutron diffraction study of pseudomonas aeruginosa lipopolysaccharide bilayers. *J. Phys. Chem. B* **2007**, *111*, 2477–2483.

(104) Snyder, S.; Kim, D.; McIntosh, T. J. Lipopolysaccharide bilayer structure: Effect of chemotype, core mutations, divalent cations, and temperature. *Biochemistry* **1999**, *38*, 10758–10767.

(105) Kućerka, N.; Papp-Szabo, E.; Nieh, M. P.; Harroun, T. A.; Schooling, S. R.; Pencer, J.; Nicholson, E. A.; Beveridge, T. J.; Katsaras, J. Effect of cations on the structure of bilayers formed by lipopolysaccharides isolated from Pseudomonas aeruginosa PAO1. *J. Phys. Chem. B* **2008**, *112*, 8057–8062.

(106) Schneck, E.; Oliveira, R. G.; Rehfeldt, F.; Deme, B.; Brandenburg, K.; Seydel, U.; Tanaka, M. Mechanical properties of interacting lipopolysaccharide membranes from

bacteria mutants studied by specular and off-specular neutron scattering. *Phys. Rev. E - Stat. Nonlinear, Soft Matter Phys.* **2009**, *80*, 1–9.

(107) Seydel, U.; Schröder, G.; Brandenburg, K. Reconstitution of the lipid matrix of the outer membrane of gram-negative bacteria as asymmetric planar bilayer. *The Journal of membrane biology* **1989**, *109*, 95–103.

(108) Gutsmann, T.; Heimburg, T.; Keyser, U.; Mahendran, K. R.; Winterhalter, M. Protein reconstitution into freestanding planar lipid membranes for electrophysiological characterization. *Nat. Protoc.* **2015**, *10*,188–198.

(109) Jeworrek, C.; Evers, F.; Howe, J.; Brandenburg, K.; Tolan, M.; Winter, R. Effects of specific versus nonspecific ionic interactions on the structure and lateral organization of lipopolysaccharides. *Biophys. J.* **2011**, *100*, 2169–2177.

(110) Blume, A. Lipids at the air–water interface. *ChemTexts* **2018**, *4*, 1–25.

(111) Ciumac, D.; Campbell, R. A.; Xu, H.; Clifton, L. A.; Hughes, A. V.; Webster, J. R.; Lu, J. R. Implications of lipid monolayer charge characteristics on their selective interactions with a short antimicrobial peptide. *Colloids and Surfaces B: Biointerfaces* **2017**, *150*, 308–316.

(112) Kurniawan, J.; Ventrici De Souza, J. F.; Dang, A. T.; Liu, G. Y.; Kuhl, T. L. Preparation and Characterization of Solid-Supported Lipid Bilayers Formed by Langmuir-Blodgett Deposition: A Tutorial. *Langmuir* **2018**, *34*, 15622–15639.

(113) Marsh, D. Lateral pressure in membranes. *Biochimica et Biophysica Acta - Reviews on Biomembranes* **1996**, *1286*,183–223.

(114) Marsh, D. Comment on Interpretation of Mechanochemical Properties of Lipid Bilayer Vesicles from the Equation of State or Pressure-Area Measurement of the Monolayer at the Air-Water or Oil-Water Interface. *Langmuir* **2006**, *22*, 2916–2919.

(115) Brandenburg, K.; Seydel, U. Physical aspects of structure and function of membranes made from lipopolysaccharides and free lipid A. *Biochimica et Biophysica Acta - Biomembranes* **1984**, *775*, 225–238.

(116) Micciulla, S.; Gerelli, Y.; Schneck, E. Structure and Conformation of Wild-Type Bacterial Lipopolysaccharide Layers at Air-Water Interfaces. *Biophys. J.* **2019**, *116*, 1259–1269.

(117) Romeo, D.; Girard, A.; Rothfield, L. Reconstitution of a functional membrane enzyme system in a monomolecular film. I. Formation of a mixed monolayer of lipopolysaccharide and phospholipid. *Journal of Molecular Biology* **1970**, *53*, 475–490.

(118) Brandenburg, K.; Seydel, U. Investigation into the fluidity of lipopolysaccharide and free lipid A membrane systems by Fourier-transform infrared spectroscopy and differential scanning calorimetry. *European Journal Of Biochemistry* **1990**, *191*, 229–236.

(119) Gidalevitz, D.; Ishitsuka, Y.; Muresan, A. S.; Konovalov, O.; Waring, A. J.; Lehrer, R. I.; Lee, K. Y. C. Interaction of antimicrobial peptide protegrin with biomem- branes. *Proceedings of the National Academy of Sciences* **2003**, *100*, 6302–6307.

(120) Oliveira, R. G.; Schneck, E.; Quinn, B. E.; Konovalov, O. V.; Brandenburg, K.; Gutsmann, T.; Gill, T.; Hanna, C. B.; Pink, D. A.; Tanaka, M. Crucial roles of charged saccharide moieties in survival of gram negative bacteria against protamine revealed by combination of grazing incidence x-ray structural characterizations and Monte Carlo simulations. *Phys. Rev. E - Stat. Nonlinear, Soft Matter Phys.* **2010**, *81*, 1–12.

(121) Neville, F.; Hodges, C. S.; Liu, C.; Konovalov, O.; Gidalevitz, D. In situ characterization of lipid A interaction with antimicrobial peptides using surface X-ray scattering. *Biochimica et biophysica acta* **2006**, *1758*, 232–240.

(122) Oliveira, R. G.; Schneck, E.; Quinn, B. E.; Konovalov, O. V.; Brandenburg, K.; Seydel, U.; Gill, T.; Hanna, C. B.; Pink, D. A.; Tanaka, M. Physical mechanisms of bacterial survival revealed by combined grazing-incidence X-ray scattering and Monte Carlo simulation. *Comptes Rendus Chim.* **2009**, *12*, 209–217.

(123) Frey, S. L.; Lee, K. Y. C. Number of sialic acid residues in ganglioside headgroup affects interactions with neighboring lipids. *Biophysical Journal* **2013**, *105*, 1421–1431.

(124) Garidel, P.; Rappolt, M.; Schromm, A. B.; Howe, J.; Lohner, K.; Andrä, J.; Koch, M. H. J.; Brandenburg, K. Divalent cations affect chain mobility and aggregate structure of lipopolysaccharide from Salmonella minnesota reflected in a decrease of its biological activity. *Biochimica et Biophysica Acta - Biomembranes* **2005**, *1715*, 122–131.

(125) Delcea, M.; Helm, C. A. X-ray and Neutron Reflectometry of Thin Films at Liquid Interfaces. *Langmuir* **2019**, *35*, 8519–8530.

(126) Gong, H.; Hu, X.; Liao, M.; Fa, K.; Clifton, L. A.; Sani, M.-A.; King, S. M.; Mae- stro, A.; Separovic, F.; Waigh, T. A.; Xu, H.; McBain, A. J.; Lu, J. R. Structural Disruptions of the Outer Membranes of Gram-Negative Bacteria by Rationally Designed Amphiphilic Antimicrobial Peptides. *ACS Applied Materials & Interfaces* **2021**,

(127) Lu, J. R.; Thomas, R.; Penfold, J. Surfactant layers at the air/water interface: structure and composition. *Advances in Colloid and Interface Science* **2000**, *84*, 143 – 304.

(128) Rodriguez-Loureiro, I.; Latza, V. M.; Fragneto, G.; Schneck, E. Conformation of Single and Interacting Lipopolysaccharide Surfaces Bearing O-Side Chains. *Biophys. J.* **2018**, *114*, 1624–1635.

(129) Ivankin, A.; Livne, L.; Mor, A.; Caputo, G. A.; Degrado, W. F.; Meron, M.; Lin, B.; Gidalevitz, D. Role of the conformational rigidity in the design of biomimetic antimicrobial compounds. *Angewandte Chemie - International Edition* **2010**, *49*, 8462–8465.

(130) Neville, F.; Ishitsuka, Y.; Hodges, C. S.; Konovalov, O.; Waring, A. J.; Lehrer, R.; Lee, K. Y. C.; Gidalevitz, D. Protegrin interaction with lipid monolayers: Grazing incidence X-ray diffraction and X-ray reflectivity study. *Soft matter* **2008**, *4*, 1665–1674.

(131) Clifton, L. A.; Skoda, M. W. A.; Brun, A. P. L.; Ciesielski, F.; Kuzmenko, I.; Holt, S. A.; Lakey, J. H. Effect of Divalent Cation Removal on the Structure of Gram-Negative Bacterial Outer Membrane Models. *Langmuir* **2015**, *31*, 404–412.

(132) Nobre, T. M.; Martynowycz, M. W.; Andreev, K.; Kuzmenko, I.; Nikaido, H.; Gidalevitz, D. Modification of Salmonella Lipopolysaccharides Prevents the Outer Membrane Penetration of Novobiocin. *Biophys. J.* **2015**, *109*, 2537–2545.

(133) Martynowycz, M. W.; Rice, A.; Andreev, K.; Nobre, T. M.; Kuzmenko, I.; Wereszczynski, J.; Gidalevitz, D. Salmonella Membrane Structural Remodeling Increases Resistance to Antimicrobial Peptide LL-37. *ACS infectious diseases* **2019**, *5*, 1214–1222.

(134) Stefaniu, C.; Latza, V. M.; Gutowski, O.; Fontaine, P.; Brezesinski, G.; Schneck, E. Headgroup-Ordered Monolayers of Uncharged Glycolipids Exhibit Selective Interactions with Ions. *Journal of Physical Chemistry Letters* **2019**, *10*, 1684–1690.

(135) Michel, J. P.; Wang, Y. X.; Dé, E.; Fontaine, P.; Goldmann, M.; Rosilio, V. Charge and aggregation pattern govern the interaction of plasticins with LPS monolayers mimicking the external leaflet of the outer membrane of Gram-negative bacteria. *Biochimica et Biophysica Acta - Biomembranes* **2015**, *1848*, 2967–2979.

(136) Zhang, L.; Dhillon, P.; Yan, H.; Farmer, S.; Hancock, R. E. W. Interactions of bacterial cationic peptide antibiotics with outer and cytoplasmic membranes of Pseudomonas aeruginosa. *Antimicrobial Agents and Chemotherapy* **2000**, *44*, 3317–3321.

(137) Retzinger, G. S.; Takayama, K. Mitogenicity of a spread film of monophosphoryl lipid A. *Experimental and Molecular Pathology* **2005**, *79*, 161–167.

(138) Clausell, A.; Garcia-Subirats, M.; Pujol, M.; Busquets, M. A.; Rabanal, F.; Cajal, Y. Gram-negative outer and inner membrane models: Insertion of cyclic cationic lipopeptides. *Journal of Physical Chemistry B* **2007**, *111*, 551–563.

(139) Abraham, T.; Schooling, S. R.; Beveridge, T. J.; Katsaras, J. Monolayer film behavior of lipopolysaccharide from Pseudomonas aeruginosa at the air-water interface. *Biomacromolecules* **2008**, *9*, 2799–2804.

(140) Ryder, M. P.; Wu, X.; McKelvey, G. R.; McGuire, J.; Schilke, K. F. Binding interactions of bacterial lipopolysaccharide and the cationic amphiphilic peptides polymyxin B and WLBU2. *Colloids and Surfaces B: Biointerfaces* **2014**, *120*, 81–87.

(141) Hwang, H.; Paracini, N.; Parks, J. M.; Lakey, J. H.; Gumbart, J. C. Distribution of mechanical stress in the Escherichia coli cell envelope. *Biochimica et Biophysica Acta (BBA) - Biomembranes* **2018**, *1860*, 2566–2575.

(142) Cetuk, H.; Anishkin, A.; Scott, A. J.; Rempe, S. B.; Ernst, R. K.; Sukharev, S. Partitioning of Seven Different Classes of Antibiotics into LPS Monolayers Supports Three Different Permeation Mechanisms through the Outer Bacterial Membrane. *Langmuir* **2021**, *37*, 1372–1385.

(143) Maget-Dana, R. The monolayer technique: A potent tool for studying the interfacial properties of antimicrobial and membrane-lytic peptides and their interactions with lipid membranes. *Biochimica et Biophysica Acta - Biomembranes* **1999**, *1462*, 109– 140.

(144) Hancock, R. E. W.; Scott, M. G. The role of antimicrobial peptides in animal defenses. *Proc. Natl. Acad. Sci. U. S. A.* **2000**, *97*, 8856–8861.

(145) Bello, G.; Bodin, A.; Lawrence, M. J.; Barlow, D.; Mason, a. J.; Barker, R. D.; Harvey, R. D. The influence of rough lipopolysaccharide structure on molecular in-

teractions with mammalian antimicrobial peptides. *Biochimica et Biophysica Acta - Biomembranes* **2016**, *1858*, 197–209.

(146) Schneck, E.; Papp-Szabo, E.; Quinn, B. E.; Konovalov, O. V.; Beveridge, T. J.; Pink, D. A.; Tanaka, M. Calcium ions induce collapse of charged O-side chains of lipopolysaccharides from Pseudomonas aeruginosa. *J. R. Soc. Interface* **2009**, *6 Suppl 5*, S671–8.

(147) Clifton, L.; Skoda, M.; Daulton, E.; a.V. Hughes,; a.P. Le Brun,; Lakey, J.; Holt, S. Asymmetric phospholipid: lipopolysaccharide bilayers; a Gram-negative bacterial outer membrane mimic. *J. R. Soc. Interface* **2013**, *10*, 20130810.

(148) Clifton, L. A.; Ciesielski, F.; Skoda, M. W.; Paracini, N.; Holt, S. A.; Lakey, J.H. The Effect of Lipopolysaccharide Core Oligosaccharide Size on the Electrostatic Binding of Antimicrobial Proteins to Models of the Gram Negative Bacterial Outer Membrane. *Langmuir* **2016**, *32*, 3485–3494.

(149) Clifton, L. A.; Holt, S. A.; Hughes, A. V.; Daulton, E. L.; Arunmanee, W.; Heinrich, F.; Khalid, S.; Jefferies, D.; Charlton, T. R.; Webster, J. R. P.; Kinane, C. J.; Lakey, J. H. An Accurate in Vitro Model of the E. coli Envelope. *Angew. Chemie - Int. Ed.* **2015**, *54*, 11952–11955.

(150) Clifton, L. A.; Campbell, R. A.; Sebastiani, F.; Campos-Terán, J.; Gonzalez-Martinez, J. F.; Björklund, S.; Sotres, J.; Cárdenas, M. Design and use of model membranes to study biomolecular interactions using complementary surface-sensitive techniques. *Adv. Colloid Interface Sci.* **2020**, *277*,102118.

(151) Merzlyakov, M.; Li, E.; Gitsov, I.; Hristova, K. Surface-supported bilayers with transmembrane proteins: Role of the polymer cushion revisited. *Langmuir* **2006**, *22*, 10145–10151.

(152) Wagner, M. L.; Tamm, L. K. Tethered polymer-supported planar lipid bilayers for reconstitution of integral membrane proteins: Silane-polyethyleneglycol-lipid as a cushion and covalent linker. *Biophysical Journal* **2000**, *79*, 1400–1414.

(153) Clifton, L.; Johnson, C. L.; Solovyova, A. S.; Callow, P.; Weiss, K. L.; Ridley, H.; Le Brun, A. P.; Kinane, C. J.; Webster, J. R. P.; Holt, S. a.; Lakey, J. H. Low resolution structure and dynamics of a colicin-receptor complex determined by neutron scattering. *Journal of Biological Chemistry* **2012**, *287*, 337–346.

(154) Oliveira, R. G.; Calderón, R. O.; Maggio, B. Surface behavior of myelin monolayers. *Biochimica et Biophysica Acta - Biomembranes* **1998**, *1370*, 127–137.

(155) Han, M. L. et al. Investigating the Interaction of Octapeptin A3 with Model Bacterial Membranes. *ACS Infect. Dis.* **2017**, *3*, 606–619.

(156) Han, M.-L.; Velkov, T.; Zhu, Y.; Roberts, K. D.; Le Brun, A. P.; Chow, S. H.; Gutu, A. D.; Moskowitz, S. M.; Shen, H.-H.; Li, J. Polymyxin-Induced Lipid A Deacylation in Pseudomonas aeruginosa Perturbs Polymyxin Penetration and Confers High-Level Resistance. *ACS chemical biology* **2018**, *13*, 121–130.

(157) Hodate, K.; Bito, Y. Temperature dependence of bactericidal action of polymyxin B. *Microbiol.Immunol.* **1982**, *26*, 737–740.

(158) Scoppola, E.; Schneck, E. Combining scattering and computer simulation for the study of biomolecular soft interfaces. *Current Opinion in Colloid & Interface Science* **2018**, *37*, 88–100.

(159) Kastowsky, M.; Gutberlet, T.; Bradaczek, H. Molecular modelling of the three-dimensional structure and conformational flexibility of bacterial lipopolysaccharide. *Journal of bacteriology* **1992**, *174*, 4798–4806.

(160) Pink, D.; Truelstrup Hansen, L.; Gill, T. A.; Quinn, B. E.; Jericho, M.; Beveridge, T. Divalent calcium ions inhibit the penetration of protamine through the polysaccharide brush of the outer membrane of Gram-negative bacteria. *Langmuir* **2003**, *19*, 8852–8858.

(161) Lins, R. D.; Straatsma, T. Computer simulation of the rough lipopolysaccharide membrane of Pseudomonas aeruginosa. *Biophysical journal* **2001**, *81*, 1037–1046.

(162) Pontes, F. J.; Rusu, V. H.; Soares, T. A.; Lins, R. D. The effect of temperature, cations, and number of Acyl chains on the lamellar to non-lamellar transition in Lipid-A membranes: A microscopic view. *J. Chem. Theory Comput.* **2012**, *8*, 3830–3838.

(163) Kirschner, K. N.; Lins, R. D.; Maass, A.; Soares, T. A. A glycam-based force field for simulations of lipopolysaccharide membranes: parametrization and validation. *Journal of chemical theory and computation* **2012**, *8*, 4719–4731.

(164) Nascimento, A.; Pontes, F. J.; Lins, R. D.; Soares, T. A. Hydration, ionic valence and cross-linking propensities of cations determine the stability of lipopolysaccharide (LPS) membranes. *Chemical communications* **2014**, *50*, 231–233.

(165) Murzyn, K.; Pasenkiewicz-Gierula, M. Structural properties of the water/membrane interface of a bilayer built of the E. coli lipid A. *The Journal of Physical Chemistry B* **2015**, *119*, 5846–5856.

(166) Kim, S.; Patel, D. S.; Park, S.; Slusky, J.; Klauda, J. B.; Widmalm, G.; Im, W. Bilayer properties of lipid A from various Gram-negative bacteria. *Biophysical journal* **2016**, *111*, 1750–1760.

(167) Brandenburg, K.; Seydel, U. Orientation measurements on membrane systems made from lipopolysaccharides and free lipid A by FT-IR spectroscopy. *European Biophysics Journal* **1988**, *16*, 83–94.

(168) Van Oosten, B.; Harroun, T. A. A MARTINI extension for Pseudomonas aeruginosa PAO1 lipopolysaccharide. *Journal of Molecular Graphics and Modelling* **2016**, *63*, 125–133.

(169) López, C. A.; Zgurskaya, H.; Gnanakaran, S. Molecular characterization of the outer membrane of Pseudomonas aeruginosa. *Biochim. Biophys. Acta - Biomembr.* **2020**, *1862*, 183151.

(170) Im, W.; Khalid, S. Molecular Simulations of Gram-Negative Bacterial Membranes Come of Age. *Annual Review of Physical Chemistry* **2020**, *71*, 171–188.

(171) Lee, J.; Patel, D. S.; Kucharska, I.; Tamm, L. K.; Im, W. Refinement of OprH-LPS Interactions by Molecular Simulations. *Biophysical Journal* **2017**, *112*, 346–355.

(172) Kesireddy, A.; Pothula, K. R.; Lee, J.; Patel, D. S.; Pathania, M.; Van Den Berg, B.; Im, W.; Kleinekathöfer, U. Modeling of Specific Lipopolysaccharide Binding Sites on a Gram-Negative Porin. *Journal of Physical Chemistry B* **2019**, *123*, 5700–5708.

(173) Domínguez-Medina, C. C. et al. Outer membrane protein size and LPS O-antigen define protective antibody targeting to the Salmonella surface. *Nat. Commun.* **2020**, *11*, 1–11.

(174) Brezesinski, G.; Schneck, E. Investigating ions at amphiphilic monolayers with X-ray fluorescence. *Langmuir* **2019**, *35*, 8531–8542.

(175) Huang, Y.; Chen, W.; Wallace, J. A.; Shen, J. All-atom continuous constant pH molecular dynamics with particle mesh Ewald and titratable water. *Journal of chemical theory and computation* **2016**, *12*, 5411–5421.

(176) Hughes, A. V.; Patel, D. S.; Widmalm, G.; Klauda, J. B.; Clifton, L.; Im, W. Physical Properties of Bacterial Outer Membrane Models: Neutron Reflectometry and Molecular Simulation. *Biophysical Journal* **2019**, *116*, 1095–1104.

(177) Jayaram, A. K.; Pappa, A. M.; Ghosh, S.; Manzer, Z. A.; Traberg, W. C.; Knowles, T. P.; Daniel, S.; Owens, R. M. Biomembranes in bioelectronic sensing. *Trends in Biotechnology* **2021**, 1–17.

(178) Kaufmann, S.; Sobek, J.; Textor, M.; Reimhult, E. Supported lipid bilayer microarrays created by non-contact printing. *Lab on a Chip* **2011**, *11*, 2403–2410.